PHYSICAL REVIEW D **84,** 056017 (2011)

Odd-parity light baryon resonances

D. Gamermann,[1,2,*] C. García-Recio,[3,4,†] J. Nieves,[5,‡] and L. L. Salcedo[3,4,§]

[1]*Cátedra Energesis de Tecnología Interdisciplinar, Universidad Católica de Valencia San Vicente Mártir, Guillem de Castro 94, E-46003, Valencia, Spain*

[2]*Instituto Universitario de Matemática Pura y Aplicada, Universidad Politécnica de Valencia, Camino de Vera 14, 46022 Valencia, Spain*

[3]*Departamento de Física Atómica, Molecular y Nuclear, Universidad de Granada, E-18071 Granada, Spain*

[4]*Instituto Carlos I de Física Teórica y Computacional, Universidad de Granada, E-18071 Granada, Spain*

[5]*Instituto de Física corpuscular (IFIC), Centro Mixto Universidad de Valencia-CSIC, Institutos de Investigación de Paterna, Aptdo. 22085, 46071, Valencia, Spain*

(Received 14 April 2011; published 30 September 2011)

We use a consistent SU(6) extension of the meson-baryon chiral Lagrangian within a coupled channel unitary approach in order to calculate the T matrix for meson-baryon scattering in the s wave. The building blocks of the scheme are the π and N octets, the ρ nonet and the Δ decuplet. We identify poles in this unitary T matrix and interpret them as resonances. We study here the nonexotic sectors with strangeness $S = 0, -1, -2, -3$ and spin $J = \frac{1}{2}, \frac{3}{2}$ and $\frac{5}{2}$. Many of the poles generated can be associated with known N, Δ, Σ, Λ, Ξ and Ω resonances with negative parity. We show that most of the low-lying three and four star odd-parity baryon resonances with spin $\frac{1}{2}$ and $\frac{3}{2}$ can be related to multiplets of the spin-flavor symmetry group SU(6). This study allows us to predict the spin-parity of the $\Xi(1620)$, $\Xi(1690)$, $\Xi(1950)$, $\Xi(2250)$, $\Omega(2250)$ and $\Omega(2380)$ resonances, which have not been determined experimentally yet.

DOI: 10.1103/PhysRevD.84.056017 PACS numbers: 11.30.Rd, 11.10.St, 11.30.Hv, 11.30.Ly

I. INTRODUCTION

To understand the structure of existing baryons has been a challenging task for many years and different approaches have been used. (See e.g. [1–11].) The interpretation of baryons as three quark states works for ground state baryons but fails in the description of many resonances. Some examples of resonances better described by other approaches are the $\Lambda(1405)$ which can be interpreted as a meson-baryon system [12–15] or the Roper resonance [16].

Since the pioneering works of Refs. [17,18], the Goldstone boson–baryon scattering, using for the dynamics constraints from chiral symmetry, has been studied in several papers. From the study of the scattering of pseudoscalars with the $J^P = \frac{1}{2}^+$ baryons in the strangenessless sector, two poles that can be associated with the $N(1535)$ and the $\Delta(1620)$ resonances were found in [19]. The $S(\text{strangeness}) = 0$, $I(\text{isospin}) = \frac{1}{2}$ subsector has also been studied in [20], where in addition to the $N(1535)$ pole, the $N(1650)$ resonance was also dynamically generated. A follow up of this work [14] analyzed the $S = -1$, $I = 0$ sector where poles associated with the $\Lambda(1405)$ and $\Lambda(1670)$ states were found and some of the findings of previous works [12,13] were also confirmed.

In [21,22] the interaction of the baryon decuplet with the pseudoscalar mesons was first studied and signatures of various $J^P = \frac{3}{2}^-$ baryon resonances were obtained. Some of these resonances are the $\Xi(1820)$, $\Lambda(1520)$ and the $\Sigma(1670)$. More recently the interaction of vector mesons with baryons is being also studied within the formalism of the hidden gauge interaction for vector mesons [23,24]. In [25] the $\rho\Delta$ interaction is studied and the authors find an explanation of why there are $J^P = \frac{1}{2}^-, \frac{3}{2}^-, \frac{5}{2}^-$ deltas nearly degenerate around 1900 MeV. Later, this work was extended in order to study all possible sectors in the interaction of the baryon decuplet with the vector meson octet [26] and many poles are obtained that can be associated with known experimental states. Also the interaction of vector mesons with the baryon octet has been studied [27,28] and again signatures of various states were found.

In principle there is no reason to expect that the interaction of pseudoscalar mesons with baryons and the interaction of vector mesons with baryons should be decoupled for channels which share S, I, and J^P (spin-parity) quantum numbers. In this work we want to explore the consequences of coupling these sectors that have been treated independently in previous works. In order to do that we use an SU(6) framework which combines spin and flavor symmetries. Thus, we will study the s-wave meson-baryon interaction, where the hadrons belong to the 35 (π octet + ρ nonet) and the 56 (N octet + Δ decuplet) SU(6) multiplets. We will use an enlarged Weinberg-Tomozawa (WT) meson-baryon Lagrangian to accommodate vector mesons and decuplet baryons, which guarantees that chiral symmetry is recovered when interactions involving

*daga1@upvnet.upv.es
†g_recio@ugr.es
‡jmnieves@ific.uv.es
§salcedo@ugr.es

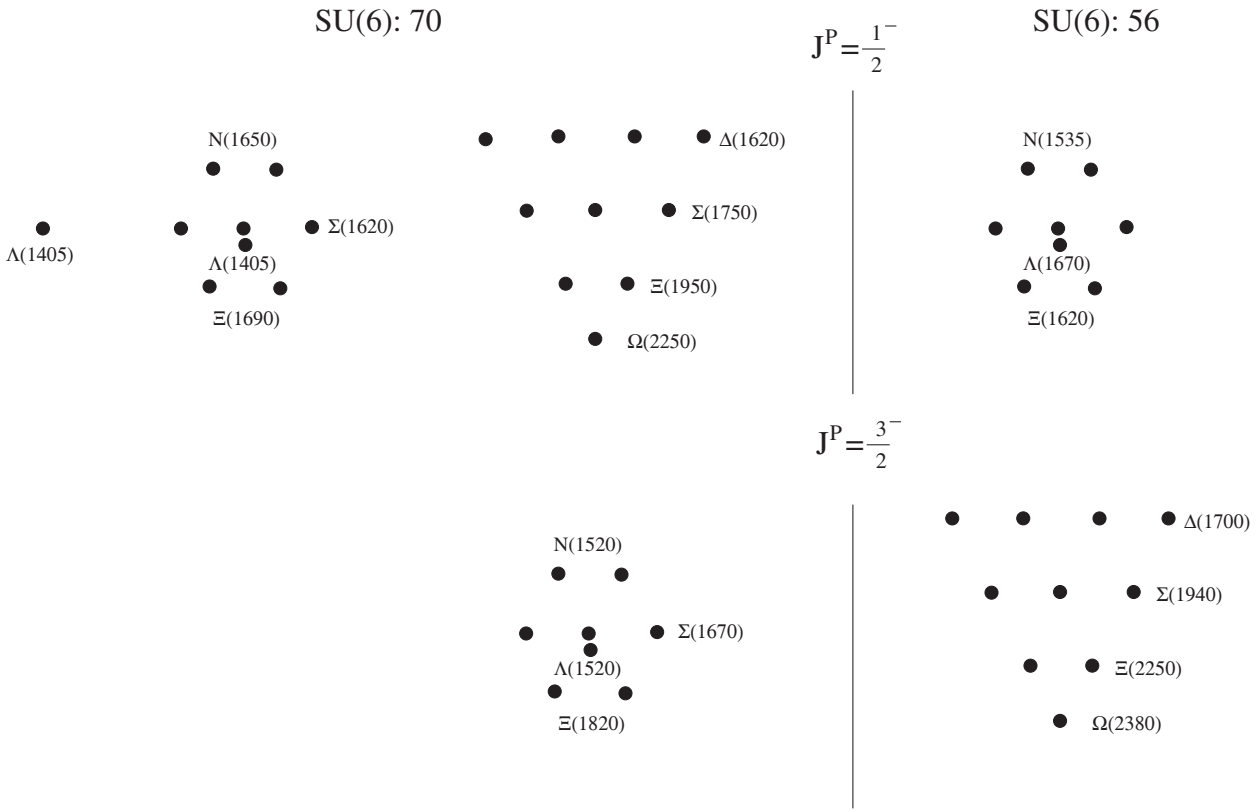

FIG. 1. Qualitative SU(6) classification derived from this work for the experimental low-lying $\frac{1}{2}^-$ and $\frac{3}{2}^-$ baryon resonances. This classification is made attending to the relation of each resonance with the different SU(6)/SU(3) multiplets that appear in the spin and/or flavor symmetric scenario described in Sec. III. Most of the odd-parity three and four star resonances of the PDG are included. Few two star ($\Sigma(1620)$, $\Xi(2250)$, and $\Omega(2380)$) and one star ($\Xi(1620)$) resonances complete the SU(6) multiplets. The only exception is the missing Σ state in the $\frac{1}{2}^-$ octet of the 56. The classification predicts the experimentally not yet known spin-parity of five resonances: $\Xi(1620)$, $\Xi(1690)$, $\Xi(1950)$, $\Xi(2250)$, $\Omega(2250)$, and $\Omega(2380)$. Most of the resonances have large SU(6) and SU(3) mixing.

pseudoscalar Nambu-Goldstone bosons are being examined.[1] Chiral symmetry constraints the pseudoscalar octet-baryon decuplet interactions, and the interactions derived here coincide with those employed in Refs. [21,22]. However, the interaction of vector mesons with baryons is not constrained by chiral symmetry, and the model presented here differs from previous ones [26,28], based in the hidden gauge formalism.

As a result of the present work, we show that most of the low-lying three and four star odd-parity baryon resonances with spin $\frac{1}{2}$ and $\frac{3}{2}$ can be related to multiplets of the spin-flavor symmetry group SU(6). This can be seen in Fig. 1, which summarizes the better theoretically founded set of dynamically generated resonances obtained in this work. The spin-parity of the $\Xi(1620)$, $\Xi(1690)$, $\Xi(1950)$, $\Xi(2250)$, $\Omega(2250)$ and $\Omega(2380)$ resonances, not experimentally determined yet,[2] can be read off the figure. The classification is qualitative. Actually, each resonance displays mixing of SU(6) and SU(3) configurations (see below).

In the next section we briefly explain the SU(6) theoretical model and the mathematical framework needed in order to calculate the T matrix and identify its poles. Also in that section, we devote a few words to clarify the differences between our scheme and that used in Refs. [26,28]. In Sec. III we present and discuss our results and in the last section we summarize our conclusions. There are also two appendices. The first one includes tables with the elementary amplitudes of the model, while in the second one, we discuss the predictions of the present model for πN phase-shifts and inelasticities in the S_{11} sector.

II. FRAMEWORK

A. The SU(6) structure of the interaction

We follow here the spin-flavor symmetric model introduced in [31–33] for meson-baryon resonances. The model is an SU(6) extension of the Weinberg-Tomozawa Lagrangian for meson-baryon interactions which assumes that the quark interactions are approximately spin and

[1] A similar study for the case of the scattering of two mesons of the 35-plet was carried out in Ref. [29].

[2] The BABAR collaboration finds some evidence that the $\Xi(1690)$ has spin-parity $1/2^-$ in [30]. Our model corroborates this assignment.

SU(3) independent. As shown in [34] (see also [29]), spin-flavor and chiral symmetries are consistent, as they can be naturally incorporated into a larger symmetry group, corresponding to the Feynman–Gell-Mann–Zweig algebra [35]. Moreover, in the presence of heavy quarks the analogous scheme automatically embodies heavy quark spin symmetry, another well established approximate symmetry of QCD. The model has been extended to the charm sector in [36,37] and to the study of meson-meson light resonances in [29].

In this SU(6) scheme, the baryons are represented by a 56-plet and the mesons by a 35-plet plus a singlet. The Lagrangian is a contact interaction obtained by coupling the mesonic current ($35 \otimes 35$) to the baryonic one ($56 \otimes 56^*$). Such coupling takes place through an implicit 35-like (i.e. adjoint representation) exchange in the t channel:

$$\mathcal{L}_{WT}^{SU(6)} \propto [[M^\dagger \otimes M]_{35_a} \otimes [B^\dagger \otimes B]_{35}]_1. \tag{1}$$

The 56-plet of baryons in SU(6) contains the spin $\frac{1}{2}^+$ and $\frac{3}{2}^+$ ground state baryons while the 35-plet of mesons contains the pseudoscalar and vector mesons. To visualize this, we show the SU(3) $\otimes$ SU(2) content of each one of these multiplets:

$$56 \rightarrow 8_2 \oplus 10_4 \tag{2}$$

$$35 \rightarrow 8_1 \oplus 8_3 \oplus 1_3. \tag{3}$$

In these equations the left-hand side indicates the SU(6) content of a multiplet and the right-hand side displays the SU(3) $\otimes$ SU(2) pattern into which it breaks. As it is standard, the regular case number indicates the SU(3) multiplet while the subindex indicates the number of spin states (the SU(2) content). So 8_2 for example is a spin $\frac{1}{2}$ (two spin states) SU(3) octet, while 8_1 represents a pseudoscalar (a single spin state) SU(3) octet.

TABLE I. SU(3) reduction of interacting multiplets.

$J = \frac{1}{2}$	$8_2 \otimes 8_1 = 1_2 \oplus 8_2 \oplus 8_2 \oplus 10_2 \oplus 10_2^* \oplus 27_2$
	$8_2 \otimes 8_3 = 1_2 \oplus 8_2 \oplus 8_2 \oplus 10_2 \oplus 10_2^* \oplus 27_2$
	$10_4 \otimes 8_3 = 8_2 \oplus 10_2 \oplus 27_2 \oplus 35_2$
	$8_2 \otimes 1_3 = 8_2$
	$10_4 \otimes 1_3 = 10_2$
$J = \frac{3}{2}$	$10_4 \otimes 8_1 = 8_4 \oplus 10_4 \oplus 27_4 \oplus 35_4$
	$10_4 \otimes 8_3 = 8_4 \oplus 10_4 \oplus 27_4 \oplus 35_4$
	$10_4 \otimes 1_3 = 10_4$
	$8_2 \otimes 8_3 = 1_4 \oplus 8_4 \oplus 8_4 \oplus 10_4 \oplus 10_4^* \oplus 27_4$
	$8_2 \otimes 1_3 = 8_4$
$J = \frac{5}{2}$	$10_4 \otimes 8_3 = 8_6 \oplus 10_6 \oplus 27_6 \oplus 35_6$
	$10_4 \otimes 1_3 = 10_6$

From the point of view of SU(6), the meson-baryon interaction is represented by the product:

$$56 \otimes 35 = 56 \oplus 70 \oplus 700 \oplus 1134. \tag{4}$$

Therefore the single 35-like coupling in the t channel (cf. Eq. (1)) corresponds to four s channel couplings. These are proportional to the following eigenvalues [31,32]:

$$\begin{aligned} \lambda_{56} &= -12, & \lambda_{70} &= -18, \\ \lambda_{700} &= 6, & \lambda_{1134} &= -2. \end{aligned} \tag{5}$$

Under SU(3) $\otimes$ SU(2) these four SU(6) multiplets break as follows:

$$56 \rightarrow 8_2 \oplus 10_4, \tag{6}$$

$$70 \rightarrow 1_2 \oplus 8_2 \oplus 10_2 \oplus 8_4, \tag{7}$$

$$700 \rightarrow 8_2 \oplus 10_2 \oplus 10_2^* \oplus 27_2 \oplus 8_4 \oplus 10_4 \oplus 27_4 \oplus 35_4 \oplus 10_6 \oplus 35_6, \tag{8}$$

$$1134 \rightarrow 1_2 \oplus 3 \times 8_2 \oplus 2 \times 10_2 \oplus 10_2^* \oplus 2 \times 27_2 \oplus 35_2 \oplus 1_4 \oplus 3 \times 8_4 \oplus 2 \times 10_4 \oplus 10_4^* \oplus 2 \times 27_4 \oplus 35_4 \oplus 8_6 \oplus 10_6 \oplus 27_6. \tag{9}$$

The SU(3) multiplets interacting for each possible value of J are displayed in Table I.

With our conventions for the potential a negative sign implies attraction. So, attending to the eigenvalues in Eq. (5), there are two strongly attractive multiplets (56 and 70), a weakly attracting one (1134) and a repulsive multiplet (700). The attractive sectors are candidates for dynamically generated resonances. This can be analyzed in terms of SU(3) multiplets and further in terms of sectors with well defined strangeness, isospin and spin.

For $J^P = \frac{1}{2}^-$, the attractive SU(3) multiplets are the 35-plet, two 27-plets, one 10^*-plet, three 10-plets, five octets and the two singlets. In the $J^P = \frac{3}{2}^-$ sector one has one 35-plet, two 27-plets, one 10^*-plet, three 10-plets, four octets and a singlet attractive and for $J^P = \frac{5}{2}^-$ there is one 27-plet, one 10-plet and one octet attractive. These

TABLE II. Expected number of states generated by the model in each sector. Here, SIJ^P stands for strangeness, isospin and spin-parity, respectively.

S	I	state	$56 \oplus 70 \oplus 1134$ J^P			$56 \oplus 70$ J^P		
			$\frac{1}{2}^-$	$\frac{3}{2}^-$	$\frac{5}{2}^-$	$\frac{1}{2}^-$	$\frac{3}{2}^-$	$\frac{5}{2}^-$
0	1/2	N	8	7	2	2	1	0
0	3/2	Δ	6	6	2	1	1	0
−1	1	Σ	12	11	3	3	2	0
−1	0	Λ	9	7	2	3	1	0
−2	1/2	Ξ	11	10	3	3	2	0
−3	0	Ω	4	4	1	1	1	0
1	0		1	1	0	0	0	0
1	1		2	2	1	0	0	0
1	2		1	1	0	0	0	0
0	5/2		1	1	0	0	0	0
−1	2		3	3	1	0	0	0
−2	3/2		4	4	1	0	0	0
−3	1		3	3	1	0	0	0
−4	1/2		1	1	0	0	0	0

attractive multiplets account for the attractive ones from the 56-plet, 70-plet and 1134-plet of Eqs. (6), (7), and (9). In Table II we show a counting of the number of states that, in principle, one can expect to generate based on the attractive multiplets of the model. As usual the particle label assigned to the state refers to its flavor quantum numbers. The states without a label in Table II are exotic in the sense that they require SU(3) irreducible representations (irreps) not present in $3 \otimes 3 \otimes 3 = 1 \oplus 8 \oplus 8 \oplus 10$. All exotic states are placed in the weakly attracting 1134 irrep, together with all spin $\frac{5}{2}^-$ and most of the $\frac{1}{2}^-$ and $\frac{3}{2}^-$ nonexotic N, Δ, Σ, Λ, Ξ and Ω ones. From Table II one expects that the model generates a very rich spectrum. This is actually the case, but not all candidate multiplets result in poles that can be associated with physical states. Some poles appear in the wrong Riemann sheet and, therefore, can not be associated with physical states. In addition, though SU(6) symmetry is the driven ingredient to fix the interaction, it is broken in the kinematics. Indeed, we implement some source of spin-flavor symmetry breaking first by using physical masses[3] for all the mesons and baryons and second by the use of different meson decay constants. Both types of symmetry breaking terms induce SU(6) violations not only at the level of kinematics, but also in the interactions. The values for the decay constants of the mesons we use are as follows (see Table II of Ref. [37]):

$$f_\pi = 92.4 \text{ MeV}, \qquad f_K = 113 \text{ MeV},$$
$$f_\eta = 111 \text{ MeV}, \qquad f_\rho = f_{K^*} = 153 \text{ MeV}, \tag{10}$$
$$f_\omega = 138 \text{ MeV}, \qquad f_\phi = 163 \text{ MeV}.$$

We assume an ideal mixing in the isoscalar vector meson sector, namely, $\omega = \sqrt{\frac{2}{3}}\omega_1 + \frac{1}{\sqrt{3}}\omega_8$ and $\phi = \sqrt{\frac{2}{3}}\omega_8 - \frac{1}{\sqrt{3}}\omega_1$.

B. Coupled channels and unitarization

All meson-baryon pairs coupled to the same SIJ quantum numbers span the coupled channel space. The s-wave tree level amplitudes between two channels for each SIJ sector are given by:

$$V_{ij}^{SIJ} = \xi_{ij}^{SIJ} \frac{2\sqrt{s} - M_i - M_j}{4 f_i f_j} \sqrt{\frac{E_i + M_i}{2M_i}} \sqrt{\frac{E_j + M_j}{2M_j}}, \tag{11}$$

where $\sqrt{s}$ is the center of mass (C.M.) energy of the system, E_i and M_i are, respectively, the C.M. energy and mass of the baryon in the channel i, f_i is the decay constant of the meson in the channel i, finally ξ_{ij}^{SIJ} are coefficients coming from the SU(6) group structure of the couplings. That is,

$$\xi_{ij}^{SIJ} = \sum_r \lambda_r [P_r]_{ij}^{SIJ}, \tag{12}$$

where $r = 56, 70, 700, 1134$, P_r denotes the projector on the SU(6) irreducible representation r and the eigenvalues λ_r are given in Eq. (5). Tables for the coefficients ξ can be found in Appendix A.

We use the matrix V^{SIJ} as a kernel to calculate the T matrix:

$$T^{SIJ} = (1 - V^{SIJ} G^{SIJ})^{-1} V^{SIJ}, \tag{13}$$

where G^{SIJ} is a diagonal matrix containing the two particle propagators for each channel. Explicitly

$$G_{ii}^{SIJ} = 2M_i(\bar{J}_0(\sqrt{s}; M_i, m_i) - \bar{J}_0(\mu^{SI}; M_i, m_i)). \tag{14}$$

m_i is the mass of the meson in the channel i. The loop function $\bar{J}_0$ can be found in the appendix of [20] for the different relevant Riemann sheets. The two particle propagator diverges logarithmically and to make it finite we have adopted the prescription of [38,39] which we now describe. The loop is renormalized by a subtraction constant such that

$$G_{ii}^{SIJ} = 0 \quad \text{at} \quad \sqrt{s} = \mu^{SI}. \tag{15}$$

To fix the subtraction point μ^{SI}, all sectors with a common SI and different J and all corresponding channels are considered. Then μ^{SI} is taken as $\sqrt{m_{\text{th}}^2 + M_{\text{th}}^2}$, where m_{th} and M_{th}, are, respectively, the masses of the meson and baryon producing the lowest threshold (minimal value of

[3]For the physical masses of the mesons we use, $m_\pi = 137.5$ MeV, $m_K = 496$ MeV, $m_\eta = 548$ MeV, $m_\rho = 775$ MeV, $m_{K^*} = 894$ MeV, $m_\omega = 783$ MeV and $m_\phi = 1019$ MeV and for the physical masses of the baryons we use, $M_N = 939$ MeV, $M_\Lambda = 1116$ MeV, $M_\Sigma = 1193$ MeV, $M_\Xi = 1318$ MeV, $M_\Delta = 1210$ MeV, $M_{\Sigma^*} = 1385$ MeV, $M_{\Xi^*} = 1533$ MeV and $M_\Omega = 1672$ MeV.

$m_{\rm th} + M_{\rm th}$). Therefore the subtraction point takes a common value for all sectors SIJ with equal SI. Results from this renormalization scheme (RS), but involving only the mesons and baryons of the pion and nucleon octets were already obtained in [15].

With all these ingredients we look for the poles of the T matrix on the $\sqrt{s}$ complex plane. Following extended practice, the poles on the first Riemann sheet on the real axis and below threshold will be called bound states. Poles on the second Riemann sheet (SRS) below the real axis and above threshold will be called resonances. Poles on the SRS on or below the real axis but below threshold will be called virtual states. Poles appearing in different positions than the ones mentioned can not be associated with physical states and are, therefore, artifacts. The real part of the pole position on the $\sqrt{s}$ complex plane is associated with the mass of the state, and the imaginary part is associated with minus one half of its width. Further information that can be extracted from the poles of the T matrix is the residue, related to the couplings of the states to their coupled channels. Close to a pole the T matrix can be written as:

$$T_{ij}^{SIJ}(z) \approx \frac{g_i g_j}{z - z_R}, \tag{16}$$

where z_R is the pole position in the $\sqrt{s}$ plane and the g_k is the dimensionless coupling of the resonance to channel k. So, by calculating the residues of the T matrix at the pole, one obtains the product of the couplings $g_i g_j$.

Some of the channels considered have mesons or baryons which are themselves resonances. The meson-baryon resonances with large couplings to these channels and with mass close to these thresholds may have their width enhanced by the decay of its components. Following [40,41], we take this effect into account by convoluting the loop function G^{SIJ} of these channels with the spectral function of the unstable particles in the channel. We use for the width of the unstable particles the values:

$$\begin{aligned} \Gamma_\rho &= 150 \text{ MeV}, \qquad \Gamma_{K^*} = 50 \text{ MeV}, \\ \Gamma_\Delta &= 120 \text{ MeV}, \qquad \Gamma_{\Sigma^*} = 35 \text{ MeV}. \end{aligned} \tag{17}$$

C. SU(6) spin flavor vs hidden gauge formalism for vector interactions

As mentioned in the introduction, the s-wave interaction of vector mesons with the octet of stable spin-parity $\frac{1}{2}^+$ baryons and with the resonances of the $\Delta(1232)$ decuplet has been previously studied in Refs. [26,28]. Both works are based on the local hidden gauge formalism for vector interactions and use a coupled channel unitary approach. In this subsection, we devote a few words to clarify the main theoretical differences between the schemes based on the hidden gauge approach and the scheme based on spin-flavor employed here. Namely

(i) Dynamics: As we commented above and explained in more detail in Ref. [31], the interaction in our model is of the form $[(35 \otimes 35)_{35_a} \otimes (56^* \otimes 56)_{35}]_1$ in the t channel. This can be regarded as the zero-range t-channel exchange of a full 35 irreducible representation of SU(6), carried by an octet of spin 0 and a nonet of spin 1 even parity mediators.
In Refs. [26,28], the interaction mechanism is the t-channel exchange of vector mesons (see diagram (b) of Fig. 2). Contributions from u- and s-channel mechanisms are neglected as they are argued to be small at threshold. Furthermore, the t-channel vector exchange is evaluated with certain approximations, which amount to neglect of both q^2/m_V^2 and the three-momentum of the external vector mesons versus their masses. In these circumstances, the interaction becomes one of contact type and it depends only on the vector meson energies, and it does not depend on three-momenta (see Eq. (9) of Ref. [26] or Eq. (12) of Ref. [28]). Actually, it is originated by the t exchange of the *time component* of vector mesons, which has certain resemblance with our zero-range exchange of 0^+ mediators.
More specifically, consider the diagram (a) of Fig. 2 near threshold where only s-wave couplings survive. Then, in any scheme, parity and angular momentum conservation implies that the pseudoscalar meson can only exchange a 0^+ mediator with the baryon. This is effectively simulated by the time component of the exchanged vector meson in the hidden gauge scheme. Our interaction and that derived from the hidden gauge Lagrangians [21,22] turn out to be identical in the pseudoscalar-baryon decuplet sector. Of course, both approaches also reduce to the SU(3) WT term in the pseudoscalar-baryon octet sector. Indeed, the interaction of soft pions with heavy sources (octet and decuplet baryons) is completely fixed by the WT theorem [42,43] (leading order in the chiral expansion) and that should be accomplished by all schemes.
Consider now the diagram (b) of Fig. 2 near threshold. In this case parity and angular momentum conservation implies that the vector meson and the

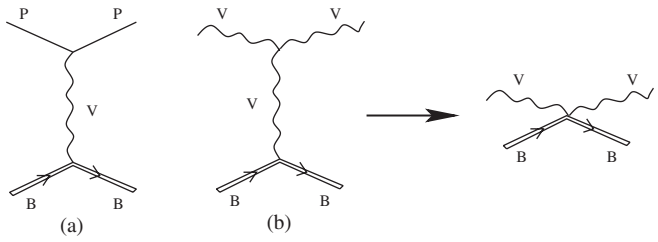

FIG. 2. Diagrams contributing to the (a) pseudoscalar-baryon or (b) vector- baryon interaction via the exchange of a vector meson leading to the effective vector-baryon contact interaction.

baryon can exchange 0^+, 1^+ and 2^+ mediators in the t channel. The 2^+ exchange is absent in our model and in that of Refs. [26,28]. The 0^+ exchange is not absent but it is similar in both schemes. The main differences between the two models arise because of the 1^+ exchange, which is present in our scheme, as required by SU(6) symmetry, while it is not present in the hidden gauge formalism adopted in Refs. [26,28]. We do not see *a priori* any compelling reason to favor either of the two approaches. It is interesting to point out that the hidden gauge vector mesons are naturally of the Proca type and so with off-shell content $(1^-, 0^+)$. Vector mesons in the antisymmetric tensor formulation have instead a $(1^-, 1^+)$ off-shell content. Such a formulation would naturally allow a 1^+ exchange in schemes based on vector meson exchange mechanisms, however, the 0^+ exchange mechanism is missing and ought to be added as a contact term. The scheme analyzed in the present work does not rely on explicit meson exchange mechanisms, instead it is based on using the minimal low energy effective interaction consistent with both chiral and spin-flavor symmetries. This yields 0^+ and 1^+ t-channel exchange mechanisms simultaneously. Nevertheless, it should be noted that chiral symmetry combined with spin-flavor favors low-lying vector mesons of the 35 of SU(6) of the antisymmetric tensor type [29,34].

(ii) Coupled channel space: Though the pseudoscalar meson-decuplet baryon $\rightarrow$ pseudoscalar meson-decuplet baryon interactions used here are the same as those employed in [21] or [22], our results will not necessarily coincide with those obtained in these two references. This is not only due to possible differences in the adopted RS or in the adopted pattern of flavor symmetry, that we will address next, but also because the coupled channel spaces are different as a consequence of the overall different dynamics. Actually, in the works of Refs. [21,22], the space does not contain channels with $J^P = \frac{3}{2}^-$ that can be constructed out of vector-decuplet or vector-octet baryon pairs. This can be extended to all sectors, for instance, interactions of the type $\rho N \rightarrow \rho\Delta$, that will connect the coupled spaces used in [26,28] are ignored in these two references. This has some effects that we will address in the next section (see for instance the discussion of the $N(1650)$ or $N(1520)$ resonances). A similar situation occurs in the context of even parity low-lying meson resonances, where the hidden gauge scheme also prevents mixings among vector-vector, vector-pseudoscalar and pseudoscalar-pseudoscalar sectors [29]. Such forbidden mixings in coupled channel space are beyond general QCD requirements and are idiosyncratic of the hidden gauge model.

(iii) Renormalization: The RS used here fixes for each IS sector the subtraction constant to some specific quantity determined by the masses of the hadrons (see Eq. (15)). This is in contrast with the RS advocated in other works [12,14,19,20,22,26,28,44], which allows for some free variations in the subtraction constants of each of the coupled channels that enter in any JIS sector.

(iv) Symmetry breaking: We use $f_V \neq f_P$ for those channels which involve vector mesons, while a universal $1/f^2$ coupling is assumed for all channels in Refs. [26,28]. Therefore the interaction involving vector mesons is weakened in our model (since $f_V > f_P$).

III. DYNAMICALLY GENERATED POLES

In order to attach each pole to definite SU(6) and SU(3) multiplets we use the following prescription. We start from an SU(6) symmetric scheme by setting the masses of all particles belonging to the same SU(6) multiplet to a common value. In this SU(6) limit we use the following values for the masses, which are approximately the average value of the mass in each multiplet, $m_{35} = 0.575$ GeV for the mesons and $M_{56} = 1.2$ GeV for the baryons. To gradually break SU(6) symmetry down to flavor SU(3) we write the mass of the hadrons as a function of a parameter x such that

$$m(x) = \bar{m} + x(m_{\mathrm{SU(3)}} - \bar{m}), \tag{18}$$

where $\bar{m} = m_{35}$, M_{56} is the mass of the hadron in the SU(6) limit and $m_{\mathrm{SU(3)}}$ is the mass of the particle in an SU(3) flavor symmetric scheme ($m_{8_1} = 0.3$ GeV and $m_{8_3} = m_{1_3} = 0.85$ GeV for the mesons and $M_{8_2} = 1$ GeV and $M_{10_4} = 1.4$ GeV for the baryons). In this way, we vary x between 0 and 1, 0 being the SU(6) limit and 1 the SU(3) limit. (Note that the modified hadron masses are also used for the subtraction points, cf. Eq. (15).) In the SU(6) limit, we also use a common value of $\bar{f} = 125$ MeV for all pseudoscalar (f_P) and vector (f_V) meson decay constants, and change f_V to gradually deviate from f_P when x increases towards 1. Namely,

$$f(x) = \bar{f} + x(f_{\mathrm{SU(3)}} - \bar{f}), \tag{19}$$

with $f_{\mathrm{SU(3)}} = f_P, f_V$, that in the flavor limit take the values $f_P = 100$ MeV and $f_V = 150$ MeV. Next, we break the SU(3) symmetry down to isospin SU(2), and now write the mass of the hadrons as a function of a parameter $y \in [0, 1]$ such that

$$m(y) = m_{\mathrm{SU(3)}} + y(m_{\mathrm{phys}} - m_{\mathrm{SU(3)}}), \tag{20}$$

where m_{phys} is the physical mass of the particle. We also change f_P and f_V to gradually approach the physical values of Eq. (10) when y reaches 1. Some states of Table II are lost (do not show up as poles in the appropriated Riemann sheets) when we move from the fully

SU(6) symmetric model to our scheme, which incorporates a certain symmetry breaking pattern. This occurs especially for states that belong to the 1134-plet.

The procedure just described is a prescription to assign SU(6) and SU(3) labels to the states. Within this prescription the only ambiguity could come from the choice of symmetric points. In any case this assignment is qualitative since the SU(6) and SU(3) symmetries are approximated ones and some mixing between irreps necessarily exists.

The WT term is a first-order s-wave potential and therefore our results could be modified to some extent by higher order terms and higher order even waves. The strong interacting multiplets, belonging to the 56-plet and 70-plet of SU(6), are tightly bound and the poles generated from these multiplets should be rather robust against perturbations caused by higher order terms. On the other hand, the poles coming from the weakly bound 1134-plet might be subject to larger relative corrections or even disappear by the consideration of such terms. In addition, resonances well above their decay threshold could receive important corrections from d-wave interactions and therefore such predictions should be less reliable. Resonances with a large d-wave component cannot be properly described within this model.

Tables III, IV, V, VI, VII, VIII, IX, X, XI, XII, XIII, XIV, XV, XVI, XVII, XVIII, XIX, and XX show the position of the resonances generated by the model in nonexotic sectors. Other properties displayed are the SU(3) and SU(6)

TABLE III. Properties for $J^P = \frac{1}{2}^-$ nucleon resonances generated by the model. The value in brackets is the new pole position after inclusion of the width of the unstable particles in the channels. An up arrow indicates the position of the pole; channels at the left of the up arrow are open for decay. The channels with largest couplings are highlighted with boldface. A question mark symbol expresses our doubts on the assignment, while states highlighted in boldface stem from the strongly attractive 70 and 56 SU(6) irreps.

SU(3) (SU(6)) irrep	Pole position [MeV]	$\lvert g_i \rvert$ πN	ηN	$K\Lambda$	$K\Sigma$	ρN	ωN	ϕN	$\rho\Delta$	$K^*\Lambda$	$K^*\Sigma$	$K^*\Sigma^*$	possible ID status PDG
27 (1134)	2160–70i	0.2	0.5	0.7	0.4	0.3	0.4	0.9	0.6	0.7	0.2	↑ **3.5**	$N(2090)$? ⋆
8 (1134)	2082–30i [2070–109i]	0.1	0.1	0.5	0.2	0.1	0.2	**1.2**	0.2	0.8	**2.6**	↑ 0.7	$N(2090)$? ⋆
8 (1134)	1795–80i [1793–98i]	0.1	0.6	0.6	**1.9**	0.5	0.4	↑ 1.1	**3.4**	1.5	1.5	0.9	
8 (1134)	1706–70i [1693–105i]	1.0	2.0	1.5	1.1	↑ 1.9	**3.2**	1.5	**3.0**	2.1	1.2	0.8	
8 (**70**)	1639–38i	1.2	0.8	0.6	↑ 1.7	0.2	**2.9**	0.7	**2.6**	1.2	0.4	1.1	**N(1650)** ⋆⋆⋆⋆
8 (**56**)	1556–47i	0.6	**2.1**	↑ 1.7	**2.4**	0.6	0.9	0.3	**2.6**	1.9	0.9	1.4	**N(1535)** ⋆⋆⋆⋆

TABLE IV. Same as Table III for $\frac{3}{2}^-$ nucleon resonances.

SU(3) (SU(6)) irrep	Pole position [MeV]	$\lvert g_i \rvert$ $\pi\Delta$	ρN	ωN	$K\Sigma^*$	ϕN	$\rho\Delta$	$K^*\Lambda$	$K^*\Sigma$	$K^*\Sigma^*$	possible ID status PDG
27 (1134)	2228–41i [2232–94i]	0.2	0.1	0.2	0.2	0.8	0.5	0.9	0.1	↑ **3.0**	$N(2080)$? ⋆⋆
10^* (1134)	2083–4i	0.1	<0.1	0.2	0.1	0.2	0.3	0.3	↑ **1.8**	0.1	$N(2080)$? ⋆⋆
8 (1134)	1895–72i [1894–106i]	0.4	1.4	0.9	1.6	↑ 1.0	**3.1**	1.1	1.1	0.3	$N(1700)$? ⋆⋆⋆
8 (1134)	1832–106i [1829–158i]	0.7	**2.1**	0.8	↑ 1.1	0.3	**3.3**	0.3	1.0	1.0	$N(1700)$? ⋆⋆⋆
8 (**70**)	1348–20i [1373–43i]	**2.4**	↑ 1.2	0.3	0.3	<0.1	**1.8**	<0.1	0.7	0.3	**N(1520)** ⋆⋆⋆⋆

TABLE V. Same as Table III for $\frac{5}{2}^-$ nucleon resonances. The (*) denotes a virtual state.

SU(3) (SU(6)) irrep	Pole position [MeV]	$\lvert g_i\rvert$ $\rho\Delta$	$K^*\Sigma^*$	possible ID status PDG
27 (1134)	2264 [2259–28i]	0	↑ **2.1**	$N(2200)$? ⋆⋆
8 (1134)	1981(*) [1994–392i]	↑ **1.6**	0	$N(2200)$? ⋆⋆

TABLE VI. Same as Table III for $\frac{1}{2}^-$ Δ resonances.

SU(3) (SU(6)) irrep	Pole position [MeV]	$\lvert g_i\rvert$ πN	$K\Sigma$	ρN	$\rho\Delta$	$\omega\Delta$	$K^*\Sigma$	$\phi\Delta$	$K^*\Sigma^*$	possible ID status PDG
35 (1134)	2244–18i [2243–45i]	0.1	0.1	0.1	0.5	0.4	0.4	0.8	↑ **2.7**	$\Delta(2150)$? ⋆
10 (1134)	2187–50i [2178–104i]	0.1	0.8	0.1	0.3	0.3	**1.4**	↑ **2.6**	**1.8**	$\Delta(2150)$? ⋆
27 (1134)	2025–88i [2028–101i]	0.1	1.7	0.1	0.7	0.6	↑ **2.7**	**2.2**	1.5	$\Delta(2150)$? ⋆
10 (1134)	1935–51i [1929–144i]	0.8	0.3	**1.3**	↑ **1.7**	**2.8**	0.4	0.3	0.3	$\Delta(1900)$? ⋆⋆
27 (1134)	1732–91i [1763–144i]	1.0	0.8	**2.1**	↑ **2.5**	**2.7**	1.4	0.8	1.6	$\Delta(1900)$? ⋆⋆
10 (**70**)	1472–77i	1.7	↑ 1.3	**2.4**	**3.7**	1.5	0.7	0.2	1.2	**Δ(1620)** ⋆⋆⋆⋆

TABLE VII. Same as Table III for $\frac{3}{2}^-$ Δ. The (*) denotes a virtual state.

SU(3) (SU(6)) irrep	Pole position [MeV]	$\lvert g_i\rvert$ $\pi\Delta$	ρN	$\eta\Delta$	$K\Sigma^*$	$\rho\Delta$	$\omega\Delta$	$K^*\Sigma$	$\phi\Delta$	$K^*\Sigma^*$	possible ID status PDG
10 (1134)	2226–17i [2214–68i]	<0.1	<0.1	0.2	0.2	<0.1	<0.1	1.0	↑ **1.9**	**1.6**	
35 (1134)	2172–49i [2170–65i]	<0.1	<0.1	0.5	1.2	0.1	<0.1	<0.1	↑ **1.9**	**2.8**	
10 (1134)	1915–40i [1912–88i]	0.8	0.2	1.0	0.4	↑ **1.6**	**2.8**	0.5	0.2	0.1	$\Delta(1940)$? ⋆
27 (1134)	1712–46i (*)	1.1	↑ 0.5	**2.3**	**2.5**	0.9	1.3	**2.9**	0.3	2.0	
10 (**56**)	1426–75i [1439–80i]	**2.3**	↑ **2.5**	0.1	0.8	1.3	0.5	1.0	1.6	0.7	**Δ(1700)** ? ⋆⋆⋆

TABLE VIII. Same as Table III for $\frac{5}{2}^-$ Δ. The (*) denotes a virtual state.

SU(3) (SU(6)) irrep	Pole position [MeV]	$\lvert g_i \rvert$ $\rho\Delta$	$\omega\Delta$	$\phi\Delta$	$K^*\Sigma^*$	possible ID status PDG
27 (1134)	2229 [2238–115i]	0	0	↑ **0.7**	**0.5**	$\Delta(2350)$? ⋆
10 (1134)	1974–15i (*) [1994–311i]	↑ **3.5**	**3.6**	0	0	$\Delta(1930)$? ⋆⋆⋆

TABLE IX. Same as Table III for $\frac{1}{2}^-$ Σ resonances.

SU(3) (SU(6)) irrep	Pole position [MeV]	$\lvert g_i \rvert$ $\pi\Lambda$	$\pi\Sigma$	$\bar{K}N$	$\eta\Sigma$	$K\Xi$	$\bar{K}^*N$	$\rho\Lambda$	$\rho\Sigma$	$\omega\Sigma$	$\bar{K}^*\Delta$	$\rho\Sigma^*$	$\omega\Sigma^*$	$K^*\Xi$	$\phi\Sigma$	$\phi\Sigma^*$	$K^*\Xi^*$	possible ID status PDG
35 (1134)	2369–16i	0.1	0.1	0.1	0.2	0.1	0.1	0.1	<0.1	<0.1	0.5	0.5	0.3	<0.1	<0.1	↑ **2.2**	**1.7**	
10 (1134)	2277–66i	0.1	<0.1	<0.1	0.6	0.4	0.1	<0.1	0.5	0.4	0.3	0.6	0.4	0.7	0.9	↑ **2.1**	**2.7**	
27 (1134)	2144–55i [2141–68i]	0.1	0.1	0.1	0.8	1.2	0.1	0.2	0.1	0.1	0.2	↑ 1.1	1.0	**1.6**	**2.1**	**1.5**	1,2	
10 (1134)	2093–48i [2090–65i]	0.6	0.3	0.6	0.2	0.4	0.6	0.8	0.4	0.1	↑ 0.3	**1.7**	**2.8**	0.4	0.6	0.4	0.6	
8 (1134)	1972–31i [1969–167i]	0.3	0.2	0.2	0.6	0.5	0.9	0.4	0.5	↑ **2.3**	**1.2**	0.3	0.5	0.8	0.8	0.5	0.5	
8 (1134)	1895–63i [1870–153i]	0.4	0.7	0.4	1.1	0.5	1.1	0.8	↑ 0.7	1.0	**2.0**	**2.1**	1.5	**2.3**	0.9	0.9	**1.9**	
8 (1134)	1867–36i [1873–53i]	0.3	0.6	0.9	0.5	0.2	0.3	↑ 1.5	0.5	1.2	**3.0**	**1.8**	0.9	1.1	0.5	0.9	1.0	
10^* (1134)	1754–74i	1.1	0.9	1.1	0.9	↑ **1.7**	**1.8**	1.3	1.0	**2.4**	0.9	1.3	0.8	**1.9**	0.7	0.2	0.7	
10 (**70**)	1599–61i	1.3	0.2	1.1	↑ 1.3	0.8	**1.9**	1.2	1.2	0.5	**3.1**	**2.4**	0.6	0.3	0.5	0.9	1.2	**Σ(1750)** ⋆⋆⋆
8 (**70**)	1489–117i	1.4	1.9	1.0	↑ 0.9	1.4	1.3	**2.3**	**2.7**	0.7	**2.1**	0.4	0.4	1.8	0.1	0.5	0.1	**Σ(1620)** ⋆⋆

multiplets assigned to them and the coupling of the resonance to each channel calculated through the residues of the poles.

For the poles which are strongly affected by the consideration of the width of unstable particles in the channels (K^*, ρ, Δ or Σ^*) we show in squared brackets the new pole position when this effect is taken into account. For each resonance an up arrow is used to indicate the position of the pole, so channels before (i.e., at the left of) the up arrow are open for decay. The main channels are indicated using boldface.

We have assigned to some poles a tentative identification with known states from the PDG [45]. This identification is made by comparing the data from the PDG on these states with the information we extract from the poles, namely, the mass, width and, most important, the couplings. The couplings give us valuable information on the structure of the state and on the possible decay channels and their relative strength. It should be stressed that there will be mixings between states with the same SIJ^P quantum numbers but belonging to different SU(6) and/or SU(3) multiplets, since these symmetries are broken both within our approach and in nature. Additional breaking of SU(6) (and SU(3)) is expected to take place not only in the kinematics but also in the interaction amplitudes. This will occur when using more sophisticated models going beyond the (hopefully dominant) lowest order retained here. No such explicit symmetry breaking has been included in our model in the interaction. Also no refitting of subtraction points is made to achieve better agreement in masses and widths of

TABLE X. Same as Table III for $\frac{3}{2}^-$ Σ resonances.

SU(3) (SU(6)) irrep	Pole position [MeV]	$\pi\Sigma^*$	$\bar{K}\Delta$	$\bar{K}^*N$	$\rho\Lambda$	$\eta\Sigma^*$	$\rho\Sigma$	$\omega\Sigma$	$K\Xi^*$	$\bar{K}^*\Delta$	$\rho\Sigma^*$	$\omega\Sigma^*$	$K^*\Xi$	$\phi\Sigma$	$\phi\Sigma^*$	$K^*\Xi^*$	possible ID status PDG
		$\lvert g_i\rvert$															
10 (1134)	2352–38i	0.1	0.2	0.2	0.1	<0.1	0.1	0.1	0.1	0.5	0.2	0.2	1.0	0.6	↑ **2.2**	**2.1**	
35 (1134)	2295–48i	<0.1	<0.1	<0.1	<0.1	0.7	<0.1	<0.1	1.0	0.1	0.1	0.1	0.1	0.1	↑ **2.4**	**2.5**	
8 (1134)	2207–2i [2210–10i]	<0.1	0.1	0.1	<0.1	0.1	0.1	0.1	0.1	0.3	0.1	0.1	↑ **1.1**	**1.3**	0.1	0.1	
27 (1134)	2150–24i [2132–107i]	0.1	<0.1	0.6	0.9	0.2	0.3	0.1	0.1	0.2	↑ **2.0**	**1.3**	<0.1	0.2	<0.1	0.1	
10 (1134)	2070–46i	0.6	0.6	0.2	0.2	0.9	0.3	0.4	0.6	↑ 0.7	**1.5**	**2.7**	0.4	0.8	<0.1	0.1	
8 (1134)	2015–46i [2001–72i]	0.4	0.9	0.5	0.3	0.5	0.6	0.8	↑ 0.9	**3.0**	0.1	0.7	0.5	**1.1**	0.6	0.4	
8 (1134)	1932–50i [1929–82i]	0.9	0.3	1.0	1.2	1.2	↑ 0.8	0.9	**1.5**	0.7	1.2	**1.4**	1.0	0.4	0.3	1.1	
10 (**56**)	1605–55i	**2.3**	↑ 1.2	**1.5**	1.9	0.7	0.9	0.3	1.1	1.1	1.3	0.6	0.7	0.6	0.5	1.0	**Σ(1940)** ? ★★★
8 (**70**)	1571–8i	1.1	↑ **3.1**	1.5	0.9	1.2	0.2	0.2	0.4	**2.7**	0.8	0.5	0.3	1.0	0.9	0.4	**Σ(1670)** ★★★★

TABLE XI. Same as Table III for $\frac{5}{2}^-$ Σ resonances.

SU(3) (SU(6)) irrep	Pole position [MeV]	$\bar{K}^*\Delta$	$\rho\Sigma^*$	$\omega\Sigma^*$	$\phi\Sigma^*$	$K^*\Xi^*$	possible ID status PDG
		$\lvert g_i\rvert$					
27 (1134)	2394 [2390–9i]	0	0	0	↑ **1.5**	**1.6**	Σ(2250) ? ★★★
10 (1134)	2159–0.0i [2162–151i]	0.1	↑ **0.9**	**0.7**	0	0.4	
8 (1134)	2100 (*) [2128–178i]	↑ **1.8**	0.6	**1.3**	0	0	

the resonances or in phase-shifts and inelasticities (we will briefly address this issue in Appendix B).

In the following we comment on the identifications made in each sector separately.

A. Nucleons (N)

Results for the nucleonlike resonances are summarized in Tables III, IV, and V, for $J^P = \frac{1}{2}^-$, $J^P = \frac{3}{2}^-$, and $J^P = \frac{5}{2}^-$ respectively.

(i) In the PDG there are three $J^P = \frac{1}{2}^-$ resonances, namely, $N(1535)$, $N(1650)$ and $N(2090)$. The existence of the first two is firmly established, while the latest George Washington University (GWU) partial-wave analysis of πN data [46] finds no evidence for the one star resonance placed above 2 GeV. Experimentally there is no information on branching fractions for the decays of this state and there is a huge uncertainty in its mass. Some analysis suggests that it could be as small as 1822 ± 43 MeV [47] or as large as 2180 ± 80 MeV [48]. Any of the two poles in Table III located in the region of 2 GeV might have some relation with this $N(2090)$, if it exists. From the theoretical point of view these two poles come from the weakly attracting 1134 irrep and we have already expressed our concerns on the real existence of states stemming from this SU(6) part of the interaction. Nonetheless in both cases, the couplings of these two poles to the open light channels are small, in special to πN, which might explain the lack of evidence of their existence in the GWU

TABLE XII. Same as Table III for $\frac{1}{2}^-$ Λ resonances.

SU(3) (SU(6)) irrep	Pole position [MeV]	$\pi\Sigma$	$\bar{K}N$	$\eta\Lambda$	$K\Xi$	$\bar{K}^*N$	$\omega\Lambda$	$\rho\Sigma$	$\phi\Lambda$	$\rho\Sigma^*$	$K^*\Xi$	$K^*\Xi^*$	possible ID status PDG
		$\lvert g_i\rvert$											
27 (1134)	2254–74i	0.2	0.2	0.6	0.6	0.6	0.3	0.2	**1.0**	0.8	0.3	↑ **3.6**	
27 (1134)	2182–27i [2177–52i]	0.2	0.1	0.2	0.4	0.3	0.3	0.8	0.5	0.3	↑ **2.8**	0.8	
8 (1134)	2104–56i	<0.1	0.1	1.2	1.0	0.4	0.1	<0.1	↑ **2.9**	0.3	1.3	**2.1**	
8 (1134)	1929–44i [1914–57i]	0.2	0.3	1.0	1.0	0.1	0.2	↑ **1.4**	0.3	**3.4**	0.2	**1.4**	
8 (1134)	1870–27i	0.8	0.2	0.5	0.5	0.1	↑ **2.4**	**1.8**	0.2	1.4	1.3	1.0	$\Lambda(1800)$? ⋆⋆⋆
1 (1134)	1826–42i [1824–115i]	0.2	**1.4**	0.2	0.4	↑ **2.5**	**1.4**	**1.4**	0.8	0.6	0.4	1.2	$\Lambda(1800)$? ⋆⋆⋆
8 (**56**)	1691–26i	0.5	0.9	0.8	↑ **2.8**	1.0	0.2	**2.5**	0.3	1.2	1.4	1.2	**$\Lambda(1670)$** ⋆⋆⋆⋆
8 (**70**)	1430–3i	0.5	↑ **1.8**	0.9	0.1	**2.2**	0.5	0.3	0.9	0.4	0.2	0.1	**$\Lambda(1405)$** ⋆⋆⋆⋆
1 (**70**)	1374–85i	**2.6**	↑ 1.0	0.2	0.5	0.6	0.2	**1.7**	0.2	0.6	0.9	0.3	**$\Lambda(1405)$** ⋆⋆⋆⋆

TABLE XIII. Same as Table III for $\frac{3}{2}^-$ Λ resonances.

SU(3) (SU(6)) irrep	Pole position [MeV]	$\pi\Sigma^*$	$\bar{K}^*N$	$\omega\Lambda$	$\rho\Sigma$	$\lvert g_i\rvert$ $K\Xi^*$	$\phi\Lambda$	$\rho\Sigma^*$	$K^*\Xi$	$K^*\Xi^*$	possible ID status PDG
27 (1134)	2338–54i	0.3	0.1	0.4	0.3	0.1	**1.2**	0.7	0.4	↑ **3.2**	$\Lambda(2325)$? ⋆
8 (1134)	2206–11i [2198–75i]	0.1	0.1	0.1	<0.1	0.3	**1.0**	0.3	↑ **2.1**	0.4	
8 (1134)	2090–65i [2076–125i]	0.2	0.8	0.6	**1.1**	**1.1**	↑ **1.0**	**2.8**	**1.0**	0.6	
1 (1134)	2023–79i [2029–144i]	0.5	0.9	0.5	**2.1**	↑ **1.6**	0.7	**2.7**	0.6	1.2	
8 (1134)	1894–120i [1890–140i]	0.7	**2.8**	↑ 1.7	1.5	1.1	0.3	**2.6**	0.5	1.0	
27 (1134)	1879–32i	1.2	0.3	↑ **2.3**	1.1	1.3	0.3	**1.6**	0.4	1.1	$\Lambda(1690)$? ⋆⋆⋆⋆
8 (**70**)	1542–37i	**2.3**	↑ 0.9	0.4	1.2	0.6	<0.1	**1.6**	0.6	0.6	**$\Lambda(1520)$** ⋆⋆⋆⋆

analysis. Moreover, they are placed very close to the $K^*\Sigma^*$ and $K^*\Sigma$ thresholds, respectively, but, precisely these poles strongly couple to these channels, having the largest couplings among all showed in Table III. From this perspective, these two poles might point out the actual existence of some physical states at these energies. The works of Refs. [26,28] also find similar states.

TABLE XIV. Same as Table III for $\frac{5}{2}^-$ Λ resonances.

SU(3) (SU(6)) irrep	Pole position [MeV]	$\lvert g_i \rvert$ $\rho\Sigma^*$	$K^*\Xi^*$	possible ID status PDG
27 (1134)	2404 [2399–11i]	0	↑ **2.4**	
8 (1134)	2160 [2167–276i]	↑ **0.6**	0	

TABLE XV. Same as Table III for $\frac{1}{2}^-$ Ξ resonances.

SU(3) (SU(6)) irrep	Pole position[MeV]	$\lvert g_i \rvert$ $\pi\Xi$	$\bar{K}\Lambda$	$\bar{K}\Sigma$	$\eta\Xi$	$\bar{K}^*\Lambda$	$\bar{K}^*\Sigma$	$\rho\Xi$	$\omega\Xi$	$\bar{K}^*\Sigma^*$	$\rho\Xi^*$	$\omega\Xi^*$	$\phi\Xi$	$\phi\Xi^*$	$K^*\Omega$	possible ID status PDG
35 (1134)	2476–28i	0.1	0.1	0.2	0.2	0.1	0.1	0.1	<0.1	0.9	0.4	0.3	0.1	↑ **2.9**	**1.1**	
10 (1134)	2338–67i	0.2	0.1	0.3	0.7	0.4	0.8	0.3	0.3	0.2	0.8	0.5	0.8	↑ **1.5**	**3.5**	
27 (1134)	2244–38i	0.3	0.5	0.3	1.2	0.4	0.2	0.3	<0.1	↑ 0.8	0.8	**2.9**	**2.5**	**1.3**	**1.3**	
10 (1134)	2238–53i [2229–71i]	0.3	0.6	0.3	1.2	0.7	0.5	0.6	0.1	↑ 0.4	**2.0**	**2.2**	**2.7**	1.0	1.5	
27 (1134)	2094–59i [2111–111i]	0.4	0.3	0.7	0.6	0.9	1.0	1.0	↑ 0.8	**1.5**	**2.1**	1.2	**1.4**	0.4	**2.5**	
8 (1134)	2037–24i	0.6	0.6	0.3	0.2	0.3	↑ 0.5	1.5	0.6	**1.8**	**2.4**	1.1	0.2	1.0	**2.1**	
10 (**70**)	1729–46i	0.6	1.4	0.4	↑ 1.6	1.4	**2.1**	1.0	0.4	**3.3**	1.5	0.4	0.2	1.6	1.0	**Ξ(1950)** ⋆⋆⋆
8 (**70**)	1651–2i	0.2	0.3	↑ **2.2**	1.3	1.0	**2.6**	0.2	0.6	0.9	0.4	0.2	**1.7**	0.4	0.2	**Ξ(1690)** ⋆⋆⋆
8 (**56**)	1577–139i	**2.6**	↑ **1.7**	0.5	0.1	0.8	1.0	0.7	0.1	0.6	1.3	0.3	0.1	0.2	1.2	**Ξ(1620)** ⋆

It seems natural to associate the 56-plet pole obtained at $\sqrt{s} = 1556 - 47i$ MeV with the $N(1535)$ resonance, since its mass and width are in close agreement with the experimental state and because the dominant decay channel observed for this resonance, the $N\eta$ channel, is the one to which the pole has a large coupling.

In the region of the $N(1650)$ resonance, our model generates two or even perhaps three poles that could be contributing to this resonance. It looks reasonable to identify the one at $\sqrt{s} = 1639 - 38i$ MeV, related to the strongly attractive 70 irrep, with the four star $N(1650)$ resonance. Actually, its mass, width and main decay modes agree reasonably well with those reported in the PDG [45]. The other two 1134 poles, if it happens that one or both of them exist, might induce some mixings, most likely difficult to disentangle from the experimental point of view. In Ref. [28], the dynamics of the state identified there as the $N(1650)$ resonance is dominated by a large ρN component, which in our case is almost negligible. In contrast, our state couples directly to the pseudoscalar meson–baryon octet πN (dominant decay mode), $K\Sigma$, $K\Lambda$ and ηN channels[4] that do not appear in the scheme of [28], and it also has a large coupling to the ωN channel, which turns out to be very small in [28]. Yet, we also notice a large coupling of our pole to the closed channel $\rho\Delta$, which is absent in the analysis of Ref. [28], as well. The πN decay mode, and the

[4]As in the recent work of Ref. [49], the $K\Sigma$ one is dominant among these types of components.

TABLE XVI. Same as Table III for $\frac{3}{2}^-$ Ξ resonances.

SU(3) (SU(6)) irrep	Pole position [MeV]	$\pi\Xi^*$	$\bar{K}\Sigma^*$	$\bar{K}^*\Lambda$	$\eta\Xi^*$	$\bar{K}^*\Sigma$	$\rho\Xi$	$\omega\Xi$	$K\Omega$	$\bar{K}^*\Sigma^*$	$\rho\Xi^*$	$\omega\Xi^*$	$\phi\Xi$	$\phi\Xi^*$	$K^*\Omega$	possible ID status PDG
		$\lvert g_i\rvert$														
10 (1134)	2440–54i	0.2	0.2	0.3	0.2	0.1	04.	0.3	0.1	0.5	0.5	0.3	**1.2**	↑ **2.0**	**2.6**	
35 (1134)	2414–45i	<0.1	<0.1	<0.1	0.9	<0.1	0.1	<0.1	0.8	0.1	0.1	<0.1	0.2	↑ **2.9**	**2.0**	
27 (1134)	2283–27i [2265–62i]	0.1	0.1	0.8	0.2	0.1	0.7	0.1	0.2	0.2	↑ **2.0**	**1.5**	0.3	0.1	0.2	
8 (1134)	2224–51i [2225–66i]	0.2	0.4	0.1	0.6	1.1	0.2	0.4	0.8	↑ 0.9	1.6	**2.2**	1.1	0.4	0.5	
10 (1134)	2193–46i [2189–48i]	0.3	**1.0**	0.1	0.2	0.7	0.2	0.3	0.3	↑ **3.0**	0.3	**1.3**	0.5	0.5	0.1	
8 (1134)	2104–58i [2123–93i]	0.4	0.2	0.4	0.7	**1.4**	**1.4**	0.2	↑ **2.0**	0.7	**1.0**	1.1	1.0	0.2	**1.4**	
27 (1134)	1972–47i	1.3	0.6	↑ 1.3	0.7	0.1	**1.6**	**1.6**	**1.8**	0.4	1.0	0.9	0.3	0.2	**1.5**	
10 (**56**)	1772–15i	1.4	↑ **2.7**	**2.0**	**2.1**	1.8	1.1	0.4	0.8	**2.3**	0.9	0.6	0.9	1.6	0.8	**Ξ(2250)**? ⋆⋆
8 (**70**)	1748–48i	**2.6**	↑ **1.6**	**1.5**	1.1	1.2	**2.1**	0.5	1.4	1.4	1.5	0.7	0.4	0.8	1.3	**Ξ(1820)** ⋆⋆⋆

TABLE XVII. Same as Table III for $\frac{5}{2}^-$ Ξ resonances.

SU(3) (SU(6)) irrep	Pole position [MeV]	$\bar{K}^*\Sigma^*$	$\rho\Xi^*$	$\omega\Xi^*$	$\phi\Xi^*$	$K^*\Omega$	possible ID status PDG
		$\lvert g_i\rvert$					
27 (1134)	2529 [2525–4i]	0	0	0	↑ **1.2**	**2.1**	
10 (1134)	2342–38i [2346–58i]	**3.0**	**1.2**	**1.4**	↑ 0	0	
8 (1134)	2304 [2316–118i]	0.2	↑ **1.3**	**0.9**	0	0	

width itself, of this pole will become larger when mechanisms like those depicted in Fig. 3, constructed out of the strong p-wave $\rho\pi\pi$ and $\Delta N\pi$ couplings, will be taken into account.

The discussion on the $N(1650)$ might serve to illustrate one of the differences between this study and the previous ones carried out in Refs. [26,28]. In the first of these two references, the vector-octet–baryon decuplet interaction is considered, and the second one deals with the vector-octet–baryon octet interaction. But, within the tree level hidden gauge scheme adopted in these two references, both sectors are disconnected. These two sectors in turn are also disconnected from the pseudoscalar octet–baryon octet one.[5] For instance in Refs. [26,28], couplings of the type $\pi N \to \rho N$ or $\rho\Delta \to \rho N$ do not exist, and thus within the scheme of these references, the πN and $\rho\Delta$ channel do not enter into the coupled channel dynamics that gives rise to the state identified in [28] as the $N(1650)$ resonance. Though in this case, the $\rho\Delta$ threshold is sufficiently above the mass of the $N(1650)$ resonance to keep small the influence of

[5]The pseudoscalar octet–baryon decuplet sector, that does not contribute to $J^P = 1/2^-$ in the s wave, is also separated from the other three sectors, and treated independently in Ref. [22] by the same group.

TABLE XVIII. Same as Table III for $\frac{1}{2}^-$ Ω resonances.

SU(3) (SU(6)) irrep	Pole position [MeV]	$\lvert g_i\rvert$ $\bar{K}\Xi$	$\bar{K}^*\Xi$	$\bar{K}^*\Xi^*$	$\omega\Omega$	$\phi\Omega$	possible ID status PDG
35 (1134)	2557–40i	0.4	0.3	**1.2**	0.2	↑ **3.4**	
10 (1134)	2364–26i	0.8	0.5	↑ 0.7	**3.0**	**1.0**	
10 (1134)	2230–62i [2245–73i]	0.4	**2.1**	↑ **3.0**	0.8	**2.0**	
10 (**70**)	1798 (*)	↑ 3.6	**5.5**	**6.8**	2.3	**4.7**	**Ω(2250)** ⋆⋆⋆

TABLE XIX. Same as Table III for $\frac{3}{2}^-$ Ω resonances.

SU(3) (SU(6)) irrep	Pole position [MeV]	$\lvert g_i\rvert$ $\bar{K}\Xi^*$	$\bar{K}^*\Xi$	$\eta\Omega$	$\bar{K}^*\Xi^*$	$\omega\Omega$	$\phi\Omega$	possible ID status PDG
35 (1134)	2519–41i	<0.1	0.1	1.1	0.1	<0.1	↑ **3.7**	
10 (1134)	2391–25i	0.1	**1.1**	0.1	↑ **1.3**	**2.5**	0.2	
10 (1134)	2322–45i	**1.2**	0.2	0.2	↑ **2.9**	0.6	0.4	
10 (**56**)	1928	↑ **1.9**	**2.4**	**2.1**	1.4	0.2	1.6	**Ω(2380)** ⋆⋆

TABLE XX. Same as Table III for $\frac{5}{2}^-$ Ω resonances.

SU(3) (SU(6)) irrep	Pole position [MeV]	$\lvert g_i\rvert$ $\bar{K}^*\Xi^*$	$\omega\Omega$	$\phi\Omega$	possible ID status PDG
10 (1134)	2416 [2415–4i]	↑ **1.1**	**2.1**	0	

this channel in the position of the pole in the SRS, this might not be the case in other sectors that we will discuss below. Nonetheless, as pointed out above, and because the large width of the ρ and Δ resonances and their large p-wave couplings to the $\pi\pi$ and πN pairs,, respectively, the $\rho\Delta$ component should enhance the πN decay mode of the $N(1650)$ resonance. The πN decay mode is reported to be large in [45] and about 80% of a total width of around 165 MeV. Note that in our case, the coupling of the $N(1650)$ resonance to the $\rho\Delta$ channel is an additional source for its πN decay mode (we have a direct sizeable coupling to πN, $g_{\pi N} = 1.2$, see Table III). In the scheme of Ref. [28], the $N^*(1650) \to \pi N$ decay should predominantly proceed through a diagram similar to that depicted in the left panel of Fig. 3, but replacing the intermediate $\Delta(1232)$ by a $N(940)$. Although, it is true that the latter baryon will be less off shell than the former one, one should also bear in mind that the p-wave coupling $\pi N\Delta$ is more than twice larger than the corresponding πNN one.

Likely, there will be also some mixing between the $J^P = \frac{1}{2}^-$ nucleon states that we have identified here as the $N(1535)$ and the $N(1650)$ resonances,

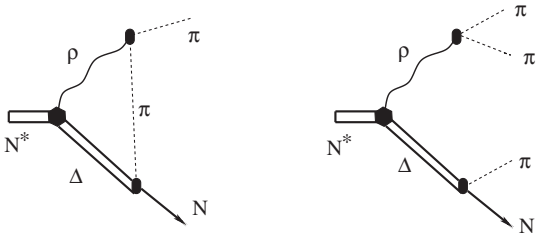

FIG. 3. Resonance (N^*) decay to πN (left) or $\pi\pi\pi N$ (right) through its s-wave (hexagon) coupling to $\Delta\rho$ and the p-wave coupling (ovals) of these latter hadrons to two pions and to a πN pair.

since they were originated by different SU(6) multiplets, and this spin–flavor symmetry is broken in nature with additional terms to those considered in the present approach.

The $N(1535)$ and $N(1650)$ resonances, neglecting the influence of the decuplet baryons and the nonet of vector mesons, were previously studied within a similar RS in Ref. [15] using the chiral SU(3) WT amplitude as a kernel to calculate the T matrix (see Eq. (13)). The results obtained in this reference for the $N(1535)$ compare rather well with those discussed here.[6] However in [15], a clear signal for the $N(1650)$ was not found. This is common for all studies that use only the tree level SU(3) WT amplitude [17–19,50]. Indeed, this latter resonance is dynamically generated in pion-nucleon scattering analysis that either use a unitarized chiral effective Lagrangian including all dimension two contact terms [49], going in this manner beyond the leading order WT term, or if the WT is taken as the kernel, when it was used within a different RS that embodies some more counterterms [20]. In this latter case, the extra counterterms mimic the effect of higher order terms in the kernel of the Bethe-Salpeter equation, and might be also related to the extra channels induced by the vector mesons and decuplet baryons included here. The inclusion of the extra counterterms, besides allowing for a reasonable description of the properties of both N^* (1535 and 1650) resonances, leads also to a reasonable description of the πN S_{11} phase shift and inelasticity from threshold to about $\sqrt{s} \sim 1.9$ GeV, together with cross-section data for $\pi^- p \to n\eta$ and $\pi^- p \to K^0\Lambda$ in the respective threshold regions [20].

It is also illustrative to pay attention to the predictions for phase shift and inelasticities deduced from the simple model presented here. In general, the model provides a poor description of these observables, though it hints to the gross features of the amplitude. This should not be surprising, since we have not fitted any parameter and we have just retained here the SU(3) WT lowest order contribution to fix the SU(6) interaction. Moreover, additional breaking of SU(6) (and SU(3)) is expected to take place not only in the kinematics but also in the interaction amplitudes. We briefly address this issue in Appendix B for the case of $(J^P = \frac{1}{2}, I = \frac{1}{2})-\pi N$ scattering, though conclusions are similar for other sectors.

(ii) For the $J^P = \frac{3}{2}^-$ resonances there are also three possible observed states quoted in the PDG, the $N(1520)$, the $N(1700)$ and the $N(2080)$. The existence of the first state is firmly established, while latest GWU partial-wave analysis of πN data [46] finds no evidence for the two star resonance $N(2080)$.

For this J^P quantum number we expect a worst description of the experimental states since our model does not take into account the d-wave pseudoscalar-baryon channels which can give important contributions on the decays of the $J^P = \frac{3}{2}^-$ resonances.

The lightest pole found in this sector at $\sqrt{s} = 1348 - 20i$ MeV, stemming from the attractive 70 SU(6) irrep, could be associated with the $N(1520)$. Our model misses here the contribution from the d wave πN which should be important for this resonance (the branching fraction quoted in [45] is around 60% for this mode) and could bring the pole closer to the experimental position. The pole found here has large couplings to the $\pi\Delta$ and ρN channels, which account for the bulk of the approximately remaining 40% of the branching fraction quoted in the PDG [45] for the $N(1520)$. The $\pi\Delta$ and the ρN channels are considered independently in Refs. [22,28], respectively. Signals for the four star $N(1520)$ resonance are found in neither the former nor the latter of these works. We believe this is because this state appears as a result of the coupled channel dynamics involving both the $\pi\Delta$ and ρN channels, which our SU(6) model provides. Note that the pseudoscalar octet-baryon decuplet interaction is determined by chiral symmetry and therefore is the same here as that used in Ref. [22]. The interaction of vector mesons with baryons is not constrained by chiral symmetry and the hidden-gauge scheme of Refs. [26,28] predicts different potentials than the ones used here and deduced from spin-flavor SU(6) symmetry. We should finally mention that in Ref. [21], this $N(1520)$ resonance was also dynamically generated with a large $\pi\Delta$ component.

[6]The $N(1535)$ alone has received a lot of attention since the pioneering work of Ref. [17,18], and several groups [19,50] have also found a fair description of its dynamics starting from the tree level SU(3) chiral Lagrangian.

The rest of the poles predicted by the SU(6) model are related to the 1134 irrep, and thus are subject to much larger uncertainties. Perhaps, the $N(1700)$ can be associated to one or both of the poles at $\sqrt{s} = 1895 - 72i$ MeV and $\sqrt{s} = 1832 - 106i$ MeV. The observed state has as the most important decay channel the $N\pi\pi$, which is a result of the decay to the $\Delta\pi$ and $N\rho$ channels to which these two poles generated by the model have important couplings.

The data on the heavier $N(2080)$ state are ambiguous and more experimental information is needed in order to do a proper association of the 1134 heavier poles displayed in Table IV with the $N(2080)$. Comments here are similar to those we made above in the case of the spin $1/2$ $N(2090)$ resonance. Nevertheless, we would like to point out that a recent study [51] finds indirect hints of the existence of the nucleon resonance $N(2080)$ in the recent data of the LEPS collaboration on the $\vec{\gamma}p \to K^+\Lambda(1520)$ reaction [52,53]. Actually in Ref. [51], it is shown that the inclusion of this resonance, with a sizable coupling to the $\Lambda(1520)K$ pair, leads to a fairly good description of a bump structure in the differential cross section at forward K^+ angles observed in the new LEPS differential cross section data [53]. The pole at $\sqrt{s} = 2228 - 41i$ MeV, related to a SU(3) 27-plet, will naturally provide a sizable $\Lambda(1520)KN(2080)$ decay thanks to: i) its dominant $K^*\Sigma^*$ coupling, ii) the large $K^* \to K\pi$ width, and iii) that, as we will discuss in the Sec. III D, the $\Lambda(1520)$ resonance has a large $\pi\Sigma^*$ component (actually, it might be a $\pi\Sigma^*$ quasi-bound state).

(iii) Two $J^P = \frac{5}{2}^-$ states are compiled in the PDG. The firmly established (four stars) $N(1675)$ resonance has a mass far too low to be associated with any of the two poles generated by our model here from the weakly bound 1134-plet. Moreover, the main decay modes of this state are the d-wave $N\pi$ and $\Delta\pi$ channels [45], which are out of the scope of our approach.

On the other hand, from the data on the unsettled two star $N(2200)$ resonance any of the two poles in Table V could be associated with it (note that the SU(6) transition potential $\rho\Delta \to K^*\Sigma^*$ is zero in this sector). The latest GWU partial-wave analysis of πN data [46] finds no evidence for this N^* resonance either.

B. Deltas (Δ)

The results for the Δ resonances are shown in Tables VI, VII, and VIII. In the PDG, there are only two firmly established four star, $\Delta(1620)$ and $\Delta(1700)$, resonances with spin-parity $\frac{1}{2}^-$ and $\frac{3}{2}^-$, respectively. In addition, there exists [45], a three star Δ state ($\Delta(1930)$) with spin-parity $\frac{5}{2}^-$, and four other resonances (two star $\Delta(1900)$ and the one star $\Delta(2150)$, $\Delta(1940)$ and $\Delta(2350)$) for which there is little evidence of their existence, as confirmed in the latest GWU partial-wave analysis of πN data [46].

(i) There are three Δ resonances in the PDG with $J^P = \frac{1}{2}^-$. To the $\Delta(1620)$ we associate the lightest pole generated by our model at $\sqrt{s} = 1472 - 77i$ MeV that comes from an SU(3) decuplet of the SU(6) 70 irrep. We see a sizeable coupling to the $N\rho$ channel and different potential sources of decay into a πN pair (direct coupling to πN and large coupling to the $\Delta\rho$ channel) in agreement with some known features of this state. However, the model misses the presumably sizable contribution that the $\pi\Delta$ d-wave channels should have in this state, and that might help to understand the difference between our prediction for its position and the mass value reported in [45]. From the data on the PDG those channels should be responsible for between 30% to 60% of the decay width of this state. The work in Refs. [26,28] does not find this $\Delta(1620)$ state. This is not surprising because here, it appears mostly as the result of the coupled channel dynamics of the πN, ρN and $\rho\Delta$ pairs, and these channels are treated separately in the framework set up in [19,22,26,28]. Unitarized chiral perturbation theory studies that do not include three-body $\pi\pi N$ states do not generate any resonance in the S_{31} partial wave at low energies either [20,49]. The effects of these latter states were taken into account, within certain approximations, in [19] and some signatures of the $\Delta(1620)$ were reported there.

The rest of the poles generated by our model in this sector are associated with the SU(6) 1134-plet, and thus deciding on their real existence and on their possible relation with physical states becomes cumbersome. This task is even more speculative given the few existing experimental evidences for the rest of the Δ states reported in the PDG. Thus, we might associate the pole at $\sqrt{s} = 1935 - 51i$ MeV with the $\Delta(1900)$ state because of the proximity in mass and width. Moreover from the PDG data the decay of this state into $N\pi$ is between 10% and 30% and the dynamically generated state has as its most important decay channels the $N\rho$ and $\Delta\rho$ channels. Yet, the pole at $\sqrt{s} = 1732 - 91i$ MeV could also be part of the $\Delta(1900)$ state or it might mix with the lightest of the poles that we identified above with the $\Delta(1620)$ resonance.

The data on the $\Delta(2150)$ is poor and either of the poles at $\sqrt{s} = 2244 - 18i$ MeV, $\sqrt{s} = 2187 - 50i$ MeV or at $\sqrt{s} = 2025 - 88i$ MeV, if they are real, could be associated with it.

(ii) For the $J^P = \frac{3}{2}^-$ Δ resonances, at first sight it might seem natural to identify the four star $\Delta(1700)$ with

the pole at $\sqrt{s} = 1712 - 46i$ MeV, although this is actually a virtual state in our model; it appears in the second Riemann sheet but below the $N\rho$ threshold. However, we rather think that the correct identification of the $\Delta(1700)$ should be done with the 56-plet pole at $\sqrt{s} = 1426 - 75i$ MeV, because of its large $\Delta\pi$ and ρN couplings. Indeed, the s-wave, $\Delta\pi$ and ρN decay modes are known to be large around 25%–50% and 5%–20%, respectively [45]. As in the case of the $\Delta(1620)$, other decay modes in the d wave (πN and also $\Delta\pi$ and ρN) are important, which points out the importance of these components in the inner structure of this resonance, and that could also explain the existing discrepancy between the pole position predicted here and that reported in [45]. Nevertheless, in this latter reference, the real part of the pole position is quoted to be well below 1700 MeV (1620 to 1680), while the resonance is quite broad, $|2\,\mathrm{Im}(\sqrt{s})| =$ 160 to 240 MeV, which makes less important the difference for the mass. This interpretation does not coincide with that of Refs. [21,22], where a second pole on top of the $\Delta\eta$ threshold and with large $\Sigma^* K$ and $\Delta\eta$ couplings was identified with the $\Delta(1700)$. This state would correspond to the virtual state found here. The wide pole placed below 1.5 GeV and with a strong coupling to the $\Delta\pi$ channel, that we have assigned here to the $\Delta(1700)$, is associated in [22] to a missing resonance, with no known counterpart in the PDG, that could be searched experimentally.

The other observed state for $J^P = \frac{3}{2}^-$ is the one star $\Delta(1940)$, which we might associate with the pole at $\sqrt{s} = 1912 - 88i$ MeV. Although there is no data on the partial decay widths of this state the mass and width of the state are fairly close to the ones obtained from the pole position.

(iii) For $J^P = \frac{5}{2}^-$, we have only structures coming from the 1134 irrep. Experimentally, there is a three star resonance $\Delta(1930)$ more or less well established and presumably with a small $N\pi$ d-wave component. It is quite wide, with a Breit-Wigner full width of around 400 MeV or larger, and it has a mass of around 1950 MeV [45]. Tentatively, we could identify the pole at $\sqrt{s} = 1994 - 311i$ MeV with the observed $\Delta(1930)$. The pole at $\sqrt{s} = 2238 - 115i$ MeV would then correspond to the $\Delta(2350)$. There is no information on the branching fractions for this state and huge uncertainty on its mass and width.

C. Sigmas (Σ)

Tables IX, X, and XI, display the results for the Σ states generated by the model. This sector is specially complex to analyze, and the situation here is unclear. On the experimental side, there are only two firmly established (four stars) odd-parity resonances. These are the $\Sigma(1670)$ and the $\Sigma(1775)$ states, with spin $3/2$ and $5/2$, respectively. The latter one cannot be described by our model, since the decays of this state reveal a fundamental role of d-wave interactions between the $N\bar{K}$, $\Lambda\pi$, $\Sigma\pi$ and $\Sigma^*\pi$ pairs. Besides these two resonances, there exists scarce trustworthy information in the PDG on s- and d-wave Σ's resonances: three additional 3-star resonances (one of them with yet undetermined J^P) and a plethora of one and two star states and undetermined spin-parity bumps from which it is difficult to draw any robust conclusion. On the theory side, there are many channels participating in the dynamics (16 and 15 for $J = \frac{1}{2}$ and $J = \frac{3}{2}$, respectively), and as a consequence, the model provides a rich spectrum in this sector. Indeed, attending to Table II, we might expect as many as 26 different states (five if we limit the study to the 56 and 70 irreps) which are difficult to identify.

(i) With $J^P = \frac{1}{2}^-$, the only state for which there is experimental information on its decays is the three star $\Sigma(1750)$ resonance. It has decays into $\bar{K}N$, $\eta\Sigma$, $\pi\Lambda$ and $\pi\Sigma$, being the latter one likely suppressed. These features seem to agree with the couplings of the pole at $\sqrt{s} = 1599 - 61i$ MeV that stems from an SU(3) decuplet of the attractive SU(6) 70 irrep. Note that from the decays compiled in [45], one might expect some d-wave $\Sigma^*\pi$ component in the structure to the $\Sigma(1750)$ resonance that is not considered within our scheme. This might, at least partially, explain the disagreement between the mass predicted by our model and that quoted in the PDG. Nevertheless, one should also bear in mind that this state is quite wide (full width $\Gamma = 60$ to 160 MeV) [45], and thus the difference in the real part of the position of the pole becomes less relevant. On the other hand, little is known on the two star $\Sigma(1620)$ state, besides it might have a width of the order of a few tens of MeV and that the $\pi\Sigma$ decay mode might be sizable. We associate to this state the lowest-lying pole ($\sqrt{s} = 1489 - 117i$ MeV) generated in our scheme and that also has its origin in the attractive 70 irrep. We find in agreement with Ref. [44] that the $\Sigma(1620)$ resonance has couplings of normal size to all pseudoscalar-baryon octet channels, and, given the large phase space available, it has a sizable decay width into any of the channels and hence a considerably large total width. Identifying any of the remaining states of Table IX, that come from the 1134 irrep, with the one star $\Sigma(2000)$ or some of the one and two star bumps listed in [45] would be too speculative and we refrain from doing it. It is noteworthy that the Σ $\frac{1}{2}^-$ state needed to complete the 56-plet does appear in the SU(6) limit, but, when going to the physical point (physical masses and

decay constants) the pole moves to unphysical regions of the $\sqrt{s}$ Riemann surface.

(ii) For $J^P = \frac{3}{2}^-$, and besides the bumps, there are three Σ states compiled in the PDG. The decay width of one of them, the four star $\Sigma(1670)$ resonance, comes mostly from d-wave pseudoscalar-baryon channels, though this state also decays into a s-wave $\Sigma^*\pi$ pair [45]. Therefore our model should have some problems predicting its mass and width correctly. Nevertheless, its $\Sigma^*\pi$ decay mode and the fact that it is relatively narrow suggests that our pole placed at $\sqrt{s} = 1571 - 8i$ MeV could be identified with this $\Sigma(1670)$ state. Indeed, this pole appears in the evolution of an SU(3) octet of the attractive 70 SU(6) irrep, and it clearly coincides (position and couplings) with that assigned to the $\Sigma(1670)$ resonance in [21,22].

The second pole generated by our model at $\sqrt{s} = 1605 - 55i$ MeV stems from an SU(3) decuplet of the 56 irrep, and it is also obtained in [22], but it is not mentioned in [21]. It is wider than the first one because it has a larger $\pi\Sigma^*$ coupling, and it is not associated with any state in [22]. Indeed, it is not straightforward to assign any state of the PDG to this pole. Its identification with the one star $\Sigma(1580)$ seems inappropriate because this state might not exist and also because in the PDG, only d-wave decay modes ($N\bar{K}$, $\Lambda\pi$ and $\Sigma\pi$) are quoted for this resonance. It could be associated with some of the bumps listed in the PDG, or perhaps this pole corresponds to the three star $\Sigma(1940)$ resonance. As we have argued before in the case of the $\Delta(1700)$, the $\Sigma(1940)$ state is very wide (full width $\Gamma = 150$ to 300 MeV) and the actual position of the pole should be influenced by genuine d-wave channels ($N\bar{K}$, $\Lambda\pi$, $\Sigma\pi$, ...) that have not been considered in the present model. The fact that this resonance has been granted with three stars [45] implies that its existence ranges from very likely to certain, which in our scheme would naturally fit with it being related to the strongly attractive 56 irrep. Furthermore, as possible decay modes of this $\Sigma(1940)$ state, the s-wave $\Sigma^*\pi$, $\bar{K}^*N$ and $\bar{K}\Delta$ pairs are also given in [45], the latter one being relatively sizable ($\sim 16\%$). This could be easily accommodated in our model if we identify the $\Sigma(1940)$ with our 56-plet pole. Instead, in Refs. [21,22], the $\Sigma(1940)$ resonance is identified with a pole much closer in mass to the 1.9 GeV region, which couples strongly to Ξ^*K, but very weakly to $\bar{K}\Delta$. This would be similar to our 1134 irrep $\sqrt{s} = 1932 - 50i$ MeV pole.

(iii) The obtained states with $J^P = \frac{5}{2}^-$ are placed in the weakly attractive 1134 irrep and are too heavy to be associated with the PDG $\Sigma(1775)$ state. Some of them or other of the 1134-plet states with $J^P = \frac{1}{2}^-$ and $J^P = \frac{3}{2}^-$, could fit some of the Σ resonances which have not had their J^P quantum numbers identified yet, but more experimental information is needed to do a proper identification. Other poles obtained here might disappear when higher order terms are taken into account in the potential.

Perhaps, the $\Sigma(2250)$ resonance is of special relevance for our discussion here. It is classified with three stars, some experiments see two resonances, one of them with $J^P = \frac{5}{2}^-$ and with a sizable ΞK decay mode [54]. Attending to this latter feature, we might assign the highest pole predicted by our model in Table XI to this $\Sigma(2250)$ state. Indeed, this is the only pole among the three compiled in this table that has a nonvanishing coupling to the $K^*\Xi^*$ channel. This decay mode would provide ΞK events through a mechanism similar to that sketched in the left panel of Fig. 3.

D. Lambdas (Λ)

Tables XII, XIII, and XIV show the results for the Λ resonances generated by the model.

(i) In the PDG there are three observed $J^P = \frac{1}{2}^-$ Λ states. The lightest of them is the $\Lambda(1405)$ which has been thoroughly studied [12–15] and is believed to have a two pole structure. In our model the two poles that describe this state are at the positions $\sqrt{s} = 1374 - 85i$ MeV and $\sqrt{s} = 1430 - 3i$ MeV, and both of them stem from the strongly attractive 70 irrep. It is noteworthy that vector mesons turn out to have important components in both poles, though channels involving these mesons are well above the position of the poles.

We identify the four star $\Lambda(1670)$ resonance with the 56 irrep pole at $\sqrt{s} = 1691 - 26i$ MeV. This state has decays to $\pi\Sigma$, $\bar{K}N$ and $\eta\Lambda$ but the couplings are not so strong and the resonance, despite the large phase space available for the decays, is fairly narrow. Indeed, this state shows a large $K\Xi$ component, but this channel is kinematically closed. Results for this resonance here compare rather well with those obtained in Refs. [14,15,44].

We also find two poles in the region of the $\Lambda(1800)$ at positions $\sqrt{s} = 1824 - 115i$ MeV and $\sqrt{s} = 1870 - 27i$ MeV. Both poles have small $\pi\Sigma$ couplings, and specially the singlet one shows large $\bar{K}N$ and $\bar{K}^*N$ components. The $\Lambda(1800)$ fits nicely with these features, and it has a broad width which covers the whole region of these two poles. Experimentally it should be very difficult to distinguish the contribution of each one of these two structures separately.

(ii) The most prominent resonance with $J^P = \frac{3}{2}^-$ is the $\Lambda(1520)$ which we associate with the pole located at

$\sqrt{s} = 1542 - 37i$ MeV. This state has important d-wave components which are not taken into account by our model. In [55] the authors develop a phenomenological coupling of the s-wave $\pi\Sigma^*$ and $K\Xi^*$ with the d-wave $\pi\Sigma$ and $\bar{K}N$ channels. In that model, a subtraction constant is fitted in order to obtain the pole with a lower mass than in our approach. This would be equivalent to changng the subtraction point in the calculation of the T matrix in the present approach which would drastically decrease also the width of the resonance.[7] Including then the d-wave channels in the model would create the appropriate width bringing the resonance properties closer to the experimental values.

The decay modes of the four star $\Lambda(1690)$ resonance are more or less equally distributed in d-wave pseudoscalar-baryon channels and three-body channels ($\Lambda\pi\pi$ and $\Sigma\pi\pi$). The three-body channels can come from s-wave channels considered by our model like $\Sigma^*\pi$ or $\rho\Sigma$ and therefore we could associate this state with the pole at $\sqrt{s} = 1879 - 32i$ MeV. Note that it would not be difficult to readjust the subtraction constant to achieve a better agreement of the position of this pole with the mass and the width of the physical $\Lambda(1690)$ state. We cannot discard here a possible mixing with the pole, close in energy, at $\sqrt{s} = 1894 - 120i$ MeV, and also generated within the 1134 irrep. However, this last pole is quite broad, significantly wider than the $\Lambda(1690)$ state, because of its large coupling to the open channel $\bar{K}^*N$. This latter decay mode does not appear in [45] for the physical $\Lambda(1690)$, which disfavors any relation of this pole with the physical state.

The association of the $\Lambda(2325)$ with the pole at $\sqrt{s} = 2338 - 54i$ MeV is based on the mass and width of the state, since there is not enough data on this resonance in order to analyze its decay channels. This is just a tentative identification, subject to all shortcomings that we have noted above for 1134-plet states.

(iii) The poles obtained with $J^P = \frac{5}{2}^-$ are too heavy to be associated with the firmly established $\Lambda(1830)$ resonance. The model fails to generate this state. This is not surprising because from the data on this resonance compiled in the PDG, one expects a fundamental role of d-wave interactions involving the $N\bar{K}$, $\Sigma\pi$ and $\Sigma^*\pi$ pairs.

[7]This is explicitly shown in Fig. 2 of Ref. [56]. There, it is also explained how the couplings to the different channels decrease when the dynamically generated pole approaches the $\pi\Sigma^*$ threshold.

E. Cascades (Ξ)

The results for the Ξ resonances generated by the model are shown in Tables XV, XVI, and XVII.

Besides the lowest-lying even parity Ξ and Ξ^* baryons, only the three star $\Xi(1820)$ resonance has its J^P quantum numbers ($\frac{3}{2}^-$) assigned in the PDG. This fact makes any identification of the poles predicted by our model with any physical state difficult. Nevertheless, the information we provide about possible poles and which states each of them couples most strongly could be a guiding line for the search of new resonance and/or for the correct assignment of spin and parity to those already compiled in [45].

(i) We find two $J^P = \frac{1}{2}^-$ poles below 1.7 GeV related to the strongly attractive 56 and 70 irreps. Here, we confirm the findings of Ref. [15] and these two states can clearly be identified to the $\Xi(1690)$ and $\Xi(1620)$ resonances, which clarifies the spin, parity and nature of these two resonances. The spin-parity assignment of the $\Xi(1690)$ found here corroborates the evidence presented in [30]. Of particular interest is the signal for the three star $\Xi(1690)$ resonance, where we find a quite small (large) coupling to the $\pi\Xi$ ($\bar{K}\Sigma$) channel, which explains the smallness of the experimental ratio, $\Gamma(\pi\Xi)/\Gamma(\bar{K}\Sigma) < 0.09$ [45] despite of the significant energy difference between the thresholds for the $\pi\Xi$ and $\bar{K}\Sigma$ channels. On the other hand the 56 irrep pole associated here with the $\Xi(1620)$ strongly couples to the $\pi\Xi$ channel. This work, and that of Ref. [15], widely improves the conclusions of Ref. [57], since we also address here the $\Xi(1690)$ resonance, and determine its spin-parity quantum numbers ($J^P = \frac{1}{2}^-$). Yet for spin-parity $\frac{1}{2}^-$, we predict another pole at $\sqrt{s} = 1729 - 46i$ MeV, and we are reasonably convinced of its existence since it is related to the 70 irrep. It is placed in a decuplet and it would be partner of the $\Delta(1620)$ and $\Sigma(1750)$ resonances. Assuming an equal spacing rule, we would expect a strangeness -2 state of around 1900 MeV that could naturally be the three star $\Xi(1950)$ resonance. Note that the predicted pole positions in the $\Delta(1620)$ and $\Sigma(1750)$ cases were also low by around 150 MeV. This identification would allow to fix the still undetermined spin-parity of this state to $\frac{1}{2}^-$. It couples strongly to the $\bar{K}^*\Sigma$ and $\bar{K}^*\Sigma^*$ (vector-baryon octet and vector-baryon decuplet), in an analogous manner to its partners in this decuplet that had big ρN and $\rho\Delta$, and $\bar{K}^*N$ and $\bar{K}^*\Delta$ components, respectively. Moreover, the $\bar{K}^*\Sigma$ and $\bar{K}^*\Sigma^*$ components of the pole will lead to the singularly seen $\bar{K}\Lambda$ decay mode, through mechanisms like the one in the left panel of Fig. 3, thanks to the large $\bar{K}^*\bar{K}\pi$, and $\pi\Sigma\Lambda$ and $\pi\Sigma^*\Lambda$ strong vertices. In Ref. [28], the $\Xi(1950)$ resonance is identified as one of the states generated there, but its dynamics is different from that deduced within our approach

since, in that work, coupled channel effects with vector meson-baryon decuplet are not considered.

The remaining $\frac{1}{2}^-$ poles predicted by the model stem from the weakly attractive 1134 irrep. Some of them might have some correspondence with some of the states compiled in the PDG, like the $\Xi(2120)$, $\Xi(2250)$, $\Xi(2370)$, $\Xi(2500)$, ..., or to states not discovered yet. However, we cannot make any meaningful statement, at this stage.

(ii) In the $J^P = \frac{3}{2}^-$ sector, we associate the 70-plet pole at $\sqrt{s} = 1748 - 48i$ MeV with the three star $\Xi(1820)$ state. As happens for other $J^P = \frac{3}{2}^-$ resonances, we expect that inclusion of the d-wave channels and fine tuning of the subtraction point could bring its position closer to the experimental value. The $\Xi(1820)$ dominant modes seem to be $\bar{K}\Lambda$ and perhaps $\pi\Xi^*$, but the branching fractions are very poorly determined ($30 \pm 15\%$ for both decay modes) [45]. Though we can easily explain the latter decay mode, we have serious problems to understand within our model the $\bar{K}\Lambda$ one. This, together with the fact that our pole is much wider[8] than the actual $\Xi(1820)$ state, reveals the important role played by d-wave components, not taken into account here, in the dynamics of this state. This situation is similar to those previously discussed for the other partners [$N(1520)$, $\Lambda(1520)$ and $\Sigma(1670)$] of the $\Xi(1820)$ in this 8_4 octet of the 70-plet. Neither in Ref. [26] nor in Ref. [28], this $\Xi(1820)$ state is discussed. However, it is studied in [21] and in [22]. In the latter work, both the decuplet and octet poles belonging to the 56 and 70 irreps, respectively, are found with couplings similar to those compiled in Table XVI. However, there the $\Xi(1820)$ is identified with the decuplet pole, because it is narrower, while the octet pole, that in [22] is four times wider than here, is ignored. This is because in the approach of Ref. [22] it did not show up in the $|T|^2$ plot of the amplitudes in the real plane, and hence the chances of observation were thought to be not too bright. The approach of Ref. [21] is based on speed plots, where two close poles cannot be disentangled, and hence the combined signature of the octet and decuplet poles was assigned there to the $\Xi(1820)$ resonance.

Next, we might try to identify in our scheme the 56 irrep pole with some other cascade resonance. It would be partner of the $\Delta(1700)$ and the $\Sigma(1940)$ resonances in an SU(3) decuplet, and we might have the same difficulties doing a proper assignment as in these two cases. Assuming an equal spacing rule, we would expect a cascade state of around 2.1 GeV. It would be quite far from the mass predicted by the model, however we have already faced up this problem for the other two members of this decuplet. In the PDG there exists one state in this region of energies. This is the one star $\Xi(2120)$ resonance, however the existence of this state is highly uncertain. Next in energy in the PDG, we find the two star $\Xi(2250)$ state. Its spin-parity is unknown, and it decays into the $\Xi\pi\pi$, $\Lambda\bar{K}\pi$ and $\Sigma\bar{K}\pi$ three-body states. These decay modes are in agreement with the large $\pi\Xi^*$, $\bar{K}\Sigma^*$ and $\bar{K}^*\Lambda$ couplings of the 56-plet pole, and we tentatively assign this $\Xi(2250)$ resonance to this pole. This fixes the spin-parity of this resonance, which is not known yet. Nevertheless, we must acknowledge that this identification is not theoretically robust, and it might well be instead that this pole should be associated with the $\Xi(1820)$-resonance or to a new Ξ state not discovered yet. The fact that it is related to the 56 irrep makes us confident that it might have some counterpart in nature.

(iii) In the $J^P = \frac{5}{2}^-$ sector, we find poles only from the 1134 SU(6) irrep. Experimentally, there exists one state, the three star $\Xi(2030)$, with $J \geq \frac{5}{2}$, and parity undetermined. It has large d-wave decays into $\bar{K}\Lambda$ and $\bar{K}\Sigma$, around 20% and 80%, respectively. As was the case with the four star $N(1675)$, $\Sigma(1775)$ and $\Lambda(1830)$ $\frac{5}{2}^-$ resonances, this well established state can not be described in our scheme and it might belong, together with the latter resonances, to an octet of genuine d-wave resonances of spin $\frac{5}{2}$. However, in [59] it is argued that this $\Xi(2030)$ state could be better accommodated in a $J^P = \frac{5}{2}^+$ octet that would include also the four star $N(1680)$, $\Sigma(1915)$ and $\Lambda(1820)$ resonances. It is also interesting to reproduce here a warning that is made in the PDG related to the $\Xi(1950)$: '... *the accumulated evidence for a* Ξ near 1950 MeV seems strong enough to include a $\Xi(1950)$ *in the main Baryon Table, but not much can be said about its properties. In fact, there may be more than one* Ξ *near this mass*'. We have identified the $\Xi(1950)$ with a spin-parity $\frac{1}{2}^-$ state related to a decuplet of the 70 irrep. However, if a second state would exist at this energy, that could be the octet partner of the $\frac{5}{2}^-$ resonances mentioned above.

Some of the poles listed in Table XVII might have some correspondence with some of the states compiled in the PDG, like the $\Xi(2120)$, $\Xi(2370)$, $\Xi(2500)$, ..., or to states not yet discovered. Some of them present similarities with states listed in Refs. [26,28]. However, as in the previous

[8]Note, however that because of the Flattè effect [58], with the opening of the $\bar{K}\Sigma^*$ channel to which the resonance couples strongly, the apparent width might be smaller than that deduced from the imaginary part of the pole position.

isospin-strangeness sectors, we cannot make any definitive statement for spin $5/2$ states.

F. Omegas (Ω)

Finally, Tables XVIII, XIX, and XX show the results for the Ω resonances generated by the model.

The strangeness -3 sector of the SU(6) model has been investigated in [60]. In this previous work, the meson decay constants for vector and pseudoscalar mesons were all taken equal. In the present work, however, the vector meson decay constants used are higher and therefore the interaction is weakened. As a result the binding of the resonances is reduced and their mass increased with respect to [60].

In this sector also the experimental data is very poor and more information is needed in order to do a proper identification of the poles obtained in our model. We will concentrate only in two states that are placed in two SU(3) decuplets associated with the strongly attractive 70 (in this case, we find a virtual state) and 56 irreps, respectively, and that we will identify to the $\Omega(2250)$ and $\Omega(2380)$ states. These resonances are not generated in the works of Refs. [26,28].

(i) For the 70 irrep pole, the spin is $\frac{1}{2}$ and from the various discussions above, this state would be partner of the $\Delta(1620)$, $\Sigma(1750)$ and $\Xi(1950)$ resonances. Following the pattern of flavor breaking, we expect its real mass to be around 2.2 GeV. Thus, we find a clear candidate in the PDG: the $\Omega(2250)$. Moreover, we can see that this resonance shares many features in common with the other resonances mentioned above. Among its main decay modes, we pay attention to the $\bar{K}\Xi^*$ one first. It is of the pseudoscalar-baryon decuplet type, and it would be similar to the $\pi\Delta$, $\pi\Sigma^*$ and $\pi\Xi^*$ modes for the $\Delta(1620)$, $\Sigma(1750)$ and $\Xi(1950)$ resonances, respectively. If all these resonances have spin $\frac{1}{2}$, these components are genuinely d wave and produce some distortion between the predicted masses and widths for these states in our scheme and the actual ones of the physical resonances. The other decay mode for the $\Omega(2250)$ resonance is the three-body one $\Xi\pi\bar{K}$, which is analogous to the $\Delta\pi\pi$ for the $\Delta(1620)$ and that can be naturally explained from the large vector-baryon octet $\bar{K}^*\Xi$ and vector-baryon decuplet $\bar{K}^*\Xi^*$ couplings of the 70-plet pole.

Thus we conclude that it is fair to identify this 70-plet pole with the $\Omega(2250)$ state, which in turn also determines the spin-parity of this resonance.

(ii) For the 56 irrep pole, the spin is $\frac{3}{2}$ and from the various discussions above, this state would be partner, in a decuplet, of the $\Delta(1700)$, $\Sigma(1940)$ and $\Xi(2250)$ resonances. From the pattern of flavor breaking, we expect its real mass to be around 2.5 GeV. In the PDG are listed two other omega resonances: the two star $\Omega(2380)$ and $\Omega(2470)$. The latter one is seen to decay into $\Omega\pi\pi$, while the main decay modes of the former one are $\Xi\pi\bar{K}$, $\bar{K}\Xi^*$ and $\bar{K}^*\Xi$ in perfect agreement with the couplings of our predicted 56-plet pole, and exhibiting some similarities with the features of the other members of this decuplet. Hence, it seems natural to identify this pole with the $\Omega(2380)$ resonance, which allows us again to determine its spin-parity. Similar poles were found in Refs. [21,22]. The dynamics of this state in these two references is different than that found here, since in both schemes the interplay with the vector-baryon decuplet $\bar{K}^*\Xi^*$ channel was not considered. While in the former work the state was not identified to any resonance, in the latter work it was tentatively assigned to the $\Omega(2250)$ baryon. For the reasons given above, we disagree with such an identification.

G. Exotics

If we look at Table II, there are many states that do not have N, Δ, Σ, Λ, Ξ or Ω quantum numbers. These are what we will call here exotic states. All of them stem from the evolution of the weakly attractive 1134 irrep. We find several poles, but they might be subject to larger relative corrections or even disappear by the consideration of higher order terms and higher order even waves, as we have been discussing for all nonexotic poles belonging to the 1134 irrep in the previous subsections. Given this uncertain scenario, we feel that we cannot draw any robust conclusion on exotic states at this point. It is, however, a valuable piece of information that exotic states are not related with the strongly attractive 70- and 56-plets. As we have seen, the bulk of $J = \frac{1}{2}, \frac{3}{2}$ odd-parity three and four star baryon resonances listed in the PDG can comfortably be associated with these two SU(6) multiplets. Moreover, we would like to draw the attention here to some of the findings of Ref. [32] when the number of colors N_c departs from 3. There it is shown that, in the 70 SU(6) irreducible space, the SU(6) extension of the WT s-wave meson-baryon interaction scales as $\mathcal{O}(1)$, instead of the well-known $\mathcal{O}(N_c^{-1})$ behavior for its SU(3) counterpart. However, the WT interaction behaves as $\mathcal{O}(N_c^{-1})$ within the 56 and 1134 meson-baryon spaces. This presumably implies that 1134 states do not appear in the large N_c QCD spectrum, since both excitation energies and widths grow with an approximate $\sqrt{N_c}$ rate.

Finally, we mention that in previous works [31,33], we advocated for the existence of some exotic states. In particular, we paid special attention to the existence of a pentaquark of spin $\frac{3}{2}$, isospin zero and strangeness $+1$. Indeed, it naturally showed up as a K^*N bound state with a mass around 1.7–1.8 GeV and it was part of an SU(3)

antidecuplet of the 1134 irrep. In these previous works, as mentioned above, the meson decay constant for vector and pseudoscalar mesons were taken as equal. In the present work, however, the vector meson decay constants used are higher and therefore the interaction is weakened. As a result, this pole disappears within the RS employed here. However, it is true that by using instead a cutoff to renormalize the ultraviolet loops, and keeping it greater than 1.3 GeV, one still finds such a state within the pattern of spin symmetry breaking assumed here.

To conclude, we cannot discard the existence of exotic states, because to a large extent this is a RS dependent issue. However we can say that the SU(6) extension of the WT presented here does not provide robust theoretical hints of their actual existence.

H. Assignation of SU(6) and SU(3) labels

As explained at the beginning of this Section, we have attached definite SU(6) and SU(3) labels to each pole found by paying attention to how this pole is generated in SU(6) or SU(3) symmetric scenarios. This procedure allows us to uncover the pattern of SU(6) or SU(3) multiplets in the final physical results, where these symmetries are broken.[9]

The previous procedure reveals the nature of the pole from the *genetic* point of view. Alternatively, one can study the *structure* of the resonance in the final scenario with broken symmetry. This can be done by analyzing the wave function of the resonance in coupled channels space. Following [61], we note that the pole condition on the T matrix[10] is equivalent to the Schrödinger equationlike condition

$$(G^{-1} - V)\psi = 0, \tag{21}$$

where G and V are matrices in coupled channel space and ψ is a column vector. The condition is on $\sqrt{s}$ for the matrix GV to have an eigenvector with eigenvalue equal to unity, namely, $GV\psi = \psi$. ψ is related to the wave function of the resonance in coupled channel space (more specifically to the wave function for small baryon-meson separation [61]).

Up to a factor, the quantities $V\psi$ (a column vector) are the coupling constants g_i (modulus and phase) appearing in the residue of the resonance pole. So these couplings give us information on the structure of the resonance, however, this is not directly the wave function, rather, $g_i = \langle i|V|\psi\rangle$ are the transition matrix elements related to the probability of formation and decay of the resonance. Working instead with the wave function[11] we can analyze the resonance from the point of view of its SU(6) and SU(3) composition. The coupled channel space baryon-meson basis is the basis attached to $56 \otimes 35$. In terms of product of representations, this is the ''uncoupled basis''. Using the appropriate scalar factors of $SU(6) \supset SU(3)_f \otimes SU(2)_J$ [62], one can express the same state in the ''coupled basis'', with well defined $SU(6) \supset SU(3)_f \otimes SU(2)_J$ labels. This gives us for instance how much of the resonance belongs to each of the SU(6) irreps 56, 70, 700 and 1134.

As it turns out, it is found that the irrep 1134 has an important weight in almost all resonances. This reflects that masses and meson decay constants break SU(6) (as well as SU(3)). In a purely random state the 1134 multiplet would be expected to dominate from statistical considerations. Valuable information follows from deviations from statistics. The analysis shows that the SU(6) irrep 700 has a small (in fact almost always negligible) role in the wave function of the resonances; presumably a consequence of the repulsive character of the interaction in that sector. It follows that all $\frac{5}{2}-$ poles are nearly 100% 1134 irrep.

After the evolution from the SU(6) and SU(3) symmetric points, we find that considerable mixing of irreps is achieved for resonances originally in the 56 or 70. The mixing takes place with the 1134 and also between 56 and 70. This is true in many cases and particularly in the Λ sector. Notably, the $(\Omega, \frac{3}{2}^-)$ with a pole at 1928 MeV is a very pure (56, 10) state with very small mixing. On the other hand, as a rule, the heavier resonances originally in the 1134 stay in that multiplet with small or no mixing.

From the point of view of classification of resonances, we stick to the prescription given above, based on how the resonance is originated. Because of the breaking of symmetry it would not make sense to expect the resonances to form clear and distinct multiplets at the end of the evolution different from the initial ones. Rather one expects to find the same multiplets plus breaking. As a rule, we find that the final structure of the resonances reflect the SU(6) and SU(3) multiplets assigned to them. There are

[9]An alternative procedure to reveal the genesis of each pole under SU(6) would be to study its response under changes of the eigenvalues λ_r in Eq. (12). The analysis can be extended to SU(3) in the obvious way.

[10]We work in a given sector of coupled channel space throughout, so we drop the sector label SIJ.

[11]There is a subtlety here since the quantity ψ obtained as above depends on conventions on how precisely G and V are normalized (all the conventions having the same poles in the plane $\sqrt{s}$). The proper definition of the wave function is such that the propagator is normalized as $G_s = (E - H_0)^{-1}$. In our case $G_i = c_i^2 G_{s,i}$ with $c_i = \sqrt{(M_i + m_i)/(m_i 16\pi^3\sqrt{s})}$ from Eqs. (66, 67) of [61] (note that our $G_i = 2M_i G^{\mathrm{FT}}$ for G^{FT} of [61]). The potential that combined with $G_s = c^{-1}Gc^{-1}$ (matrix notation) gives the same poles, is $V_s = cVc$, with corresponding T matrix $T_s = cTc$. The couplings from the residues of T_s at the poles are $g_s = cg$. For the (unnormalized) wave function, $g_s = V_s\psi_s$, so $\psi_s = G_s g_s = c^{-1}Gg = c^{-1}\psi$. Therefore, up to normalization, the wave function is $\sqrt{m_i/(m_i + M_i)}G_i g_i$, with G_i evaluated at the pole.

some exceptions. Thus, the pole $(1867 - 36i)$ MeV in the $(\Sigma, \frac{1}{2}^-)$ sector has a dominant structure of $(56, 8_2)$ rather than $(1134, 8_2)$. And the following poles in the $(\Xi, \frac{1}{2}^-)$ sector: $(1577 - 139i)$ and $(2037 - 24i)$ MeV would have structures of $(1134, 8_2)$ and $(56, 8_2)$, respectively. It is interesting that the large coupling of $(1577 - 139i)$ MeV to the channel $\pi\Xi$, attending to the corresponding Clebsh-Gordan coefficients, cannot be easily achieved through the 56 or 70 irreps and requires the important weight of the 1134. This pole is identified as $\Xi(1620)$, and the same large coupling is obtained in other models [15,57].

IV. SUMMARY

We have studied the light baryon resonances based on the SU(6) model introduced in [31,32]. The model assumes that the light-quark interactions are approximately spin and SU(3) flavor independent. With this assumption the usual SU(3) Weinberg-Tomozawa interaction is extended to SU(6). This allows us to construct the elementary amplitudes for the s-wave scattering of mesons with baryons including in a systematic way low-lying 0^- and 1^- mesons and $1/2^+$ and $3/2^+$ baryons. With these amplitudes, the T matrix is calculated and poles are identified. Each pole is associated with a resonance. The information obtained for each pole includes its mass, width and couplings of each resonance and comparison of the information obtained allows us to associate some of the theoretical states from the model with observed experimental states.

We have studied the possible N, Δ, Σ, Λ, Ξ and Ω states generated by the model. Most of the experimental $J^P = \frac{1}{2}^-$ states fit within our approach fairly well. For the $J^P = \frac{3}{2}^-$ one should bear in mind that d-wave channels, which are not considered in the model, might play an important role, but even with this handicap, the model describes many of the observed states. Most of the low-lying three and four star odd-parity baryon resonances with spin $\frac{1}{2}$ and $\frac{3}{2}$ are generated in our scheme, and they can be related to the 70 and 56 multiplets of the spin-flavor symmetry group SU(6), as sketched in Fig. 1. Indeed, the spin-flavor WT interaction turns out to be quite attractive in these two irreps, especially in the first one, and thus we believe these results are robust, except perhaps for those concerning the spin $\frac{1}{2}^-$ octet of the 56-plet which are subject to larger uncertainties, as argued in the previous subsections. The spin-parity of the $\Xi(1620)$, $\Xi(1690)$, $\Xi(1950)$, $\Xi(2250)$, $\Omega(2250)$ and $\Omega(2380)$ resonances, not experimentally determined yet, can be read off the figure and thus are predictions of our scheme. More precise experiments on this issue would be very welcome in order to test these assignments.

It should be stressed that we have chosen not to adjust any parameter; the RS used here completely fixes the subtraction constant to some specific quantity determined by the masses of the hadrons in each IS sector (see Eq. (15)). This is in contrast with the RS advocated in other works [12,14,19,20,22,26,28,44], which allows for some free variation in the subtraction constants of each of the coupled channels that enter in any JIS sector. Such freedom makes it possible to achieve a better phenomenological description of data. However in some sense, this flexibility dilutes the predictive power of the scheme, and also it might happen that some more freedom than that allowed by the underlying symmetry is being used.

We predict also many states associated with the weakly attractive 1134 irrep, some of them with exotic quantum numbers. In order to do a proper identification in these cases, it is essential to have accurate data because slight changes in the RS might change drastically the position and main features of the predicted states, and some of them might even disappear. That is the reason why we have tried to associate these poles with resonances in the PDG only in a few cases, mostly for those which could be related to firmly established resonances (three or four stars). In this context, we mention here that the four star $\Lambda(1690)$ and the three star $N(1700)$, $\Delta(1930)$ and $\Lambda(1800)$ resonances could also be accommodated within the model. Thus, considering the states included in Fig. 1 and these four resonances above, all three and four star odd-parity baryons listed in the PDG, except for the $N(1675)$, $\Sigma(1775)$, $\Lambda(1830)$ and $\Xi(2030)$ resonances, are dynamically generated within this scheme. These latter five states have spin $J = \frac{5}{2}$, their existence is firmly established, and in all cases their dominant decay modes always involve d-wave interactions, which are beyond the scope of this work. We observe that they can be cast into an SU(3) octet, though some other possibilities cannot be discarded.

The hidden gauge scheme of Refs. [26,28] leads to a distinctive pattern, where the higher energy states are degenerate in spin [25,26,28]. The authors of these works found in some cases candidates in the PDG that seem to follow this pattern, for instance, the triplet of resonances $\Delta(1900)$, $\Delta(1940)$, $\Delta(1930)$ that have spin-parity $J^P = \frac{1}{2}^-$, $\frac{3}{2}^-$, and $\frac{5}{2}-$, respectively.[12] Many of the states predicted in [25,26,28] are missing, however this does not mean that the pattern deduced there is necessarily incorrect, since the predicted states are at the frontier of the experimental research. It would not be difficult to fine tune the subtraction constants of some of the 1134 states, which have always energies higher than those associated with the more attractive 56 and 70 irreps, obtained in our model to meet the results of [26,28]. Indeed, in Tables VI, VII, and VIII, we have identified the triplet

[12]Note the scarce experimental evidence on the actual existence of the first two Δ states that are classified in the PDG as one and two stars, respectively.

of Δs mentioned above without introducing to modifications in the RS.

As noted, the 1134-plet contains exotic states which require pentaquark configurations. On the contrary, spin-flavor wavefunctions in the 56- and 70-plets can be obtained with qqq states, i.e., from the product $6 \otimes 6 \otimes 6$. The 70^-, which has the strongest attraction in our model and becomes dominant in the large N_c limit [32], is also natural in quark-model approaches with qqq configurations [63]. The 70^- corresponds to the symmetric combination with two quarks in s-wave (the lowest) state and the other quark in an excited p-wave state of the bag. (The color wave function is antisymmetric and so the spin-flavor-orbital wave function must be symmetric.) In this view, one would expect some mixing between our dynamically generated states and the qqq states. The situation is different for the 56^- states. For a 56 the qqq spin-flavor wave function is completely symmetric and this requires a completely symmetric wave function in the orbital space. The states obtained from putting one of the quarks in a p wave are spurious and disappear after center of mass projection. Hence 56^- is not natural as a qqq state as it requires more complicated, and so heavier, quark configurations.

ACKNOWLEDGMENTS

We thank M. Pavón Valderrama for useful discussions. Research was supported by DGI under Contract No. FIS2008-01143, Junta de Andalucía Grant No. FQM-225, Generalitat Valenciana Contract No. PROMETEO/2009/0090, the Spanish Consolider-Ingenio 2010 Programme CPAN Contract No. CSD2007-00042, and the European Community-Research Infrastructure Integrating Activity Study of Strongly Interacting Matter (HadronPhysics2, Grant Agreement No. 227431) under the 7th Framework Programme of EU.

APPENDIX A: MATRIX ELEMENTS BETWEEN SU(3) ⊗ SU(2) MULTIPLETS

This appendix presents Tables XXI, XXII, XXIII, XXIV, XXV, XXVI, XXVII, XXVIII, XXIX, XXX, XXXI, XXXII, XXXIII, XXXIV, XXXV, and XXXVI for the matrix elements ξ of Eq. (11). Because there are in all 38 sectors S, I, J (counting only those with negative eigenvalues; see Table II) and some of them with many channels, we provide here tables for the 16 (R, J) sectors where R denotes an SU(3) irreducible representation. The tables display the matrix elements between SU(3) multiplets. To obtain the matrix element for a concrete channel one should use the well-known $\mathrm{SU}(3) \supset \mathrm{SU}(2)_I \otimes \mathrm{U}(1)_Y$ isoscalar factors. We note that the tables have been constructed using the phase convention in [64] which, unlike that of [65], is suitable for more than three flavors. The corresponding isoscalar factors using this convention can

TABLE XXI. Matrix elements for **1** and $J = 1/2$. Eigenvalues: -18, -2.

$\mathbf{1_2}$	$(\mathbf{8_2}, \mathbf{8_1})$	$(\mathbf{8_2}, \mathbf{8_3})$
$(\mathbf{8_2}, \mathbf{8_1})$	-6	$4\sqrt{3}$
$(\mathbf{8_2}, \mathbf{8_3})$	$4\sqrt{3}$	-14

TABLE XXII. Matrix elements for **1** and $J = 3/2$. Eigenvalue: -2.

$\mathbf{1_4}$	$(\mathbf{8_2}, \mathbf{8_3})$
$(\mathbf{8_2}, \mathbf{8_3})$	-2

TABLE XXIII. Matrix elements for **8** and $J = 1/2$. Eigenvalues: -18, -12, 6, -2, -2, -2.

$\mathbf{8_2}$	$(\mathbf{8_2}, \mathbf{8_1})_s$	$(\mathbf{8_2}, \mathbf{8_1})_a$	$(\mathbf{8_2}, \mathbf{8_3})_s$	$(\mathbf{8_2}, \mathbf{8_3})_a$	$(\mathbf{8_2}, \mathbf{1_3})$	$(\mathbf{10_4}, \mathbf{8_3})$
$(\mathbf{8_2}, \mathbf{8_1})_s$	-3	0	$2\sqrt{3}$	$-\sqrt{15}$	0	$-2\sqrt{6}$
$(\mathbf{8_2}, \mathbf{8_1})_a$	0	-3	$-\sqrt{15}$	$2\sqrt{3}$	0	0
$(\mathbf{8_2}, \mathbf{8_3})_s$	$2\sqrt{3}$	$-\sqrt{15}$	$-\frac{7}{3}$	$\frac{4\sqrt{5}}{3}$	$-\frac{4\sqrt{10}}{3}$	$-\frac{4\sqrt{2}}{3}$
$(\mathbf{8_2}, \mathbf{8_3})_a$	$-\sqrt{15}$	$2\sqrt{3}$	$\frac{4\sqrt{5}}{3}$	$-\frac{23}{3}$	$\frac{8\sqrt{2}}{3}$	$-\frac{2\sqrt{10}}{3}$
$(\mathbf{8_2}, \mathbf{1_3})$	0	0	$-\frac{4\sqrt{10}}{3}$	$\frac{8\sqrt{2}}{3}$	$-\frac{4}{3}$	$\frac{4\sqrt{5}}{3}$
$(\mathbf{10_4}, \mathbf{8_3})$	$-2\sqrt{6}$	0	$-\frac{4\sqrt{2}}{3}$	$-\frac{2\sqrt{10}}{3}$	$\frac{4\sqrt{5}}{3}$	$-\frac{38}{3}$

TABLE XXIV. Matrix elements for **8** and $J = 3/2$. Eigenvalues: -18, 6, -2, -2, -2.

$\mathbf{8_4}$	$(\mathbf{8_2}, \mathbf{8_3})_s$	$(\mathbf{8_2}, \mathbf{8_3})_a$	$(\mathbf{8_2}, \mathbf{1_3})$	$(\mathbf{10_4}, \mathbf{8_1})$	$(\mathbf{10_4}, \mathbf{8_3})$
$(\mathbf{8_2}, \mathbf{8_3})_s$	$-\frac{10}{3}$	$-\frac{2\sqrt{5}}{3}$	$\frac{2\sqrt{10}}{3}$	$2\sqrt{3}$	$-\frac{4\sqrt{5}}{3}$
$(\mathbf{8_2}, \mathbf{8_3})_a$	$-\frac{2\sqrt{5}}{3}$	$-\frac{2}{3}$	$-\frac{4\sqrt{2}}{3}$	0	$-\frac{10}{3}$
$(\mathbf{8_2}, \mathbf{1_3})$	$\frac{2\sqrt{10}}{3}$	$-\frac{4\sqrt{2}}{3}$	$\frac{2}{3}$	0	$\frac{10\sqrt{2}}{3}$
$(\mathbf{10_4}, \mathbf{8_1})$	$2\sqrt{3}$	0	0	-6	$2\sqrt{15}$
$(\mathbf{10_4}, \mathbf{8_3})$	$-\frac{4\sqrt{5}}{3}$	$-\frac{10}{3}$	$\frac{10\sqrt{2}}{3}$	$2\sqrt{15}$	$-\frac{26}{3}$

TABLE XXV. Matrix elements for **8** and $J = 5/2$. Eigenvalue: -2.

$\mathbf{8_6}$	$(\mathbf{10_4}, \mathbf{8_3})$
$(\mathbf{10_4}, \mathbf{8_3})$	-2

TABLE XXVI. Matrix elements for **10** and $J = 1/2$. Eigenvalues: -18, 6, -2, -2.

$\mathbf{10}_2$	$(\mathbf{8}_2, \mathbf{8}_1)$	$(\mathbf{8}_2, \mathbf{8}_3)$	$(\mathbf{10}_4, \mathbf{8}_3)$	$(\mathbf{10}_4, \mathbf{1}_3)$
$(\mathbf{8}_2, \mathbf{8}_1)$	0	$-2\sqrt{3}$	$-4\sqrt{3}$	0
$(\mathbf{8}_2, \mathbf{8}_3)$	$-2\sqrt{3}$	$-\frac{4}{3}$	$-\frac{4}{3}$	$\frac{8}{3}$
$(\mathbf{10}_4, \mathbf{8}_3)$	$-4\sqrt{3}$	$-\frac{4}{3}$	$-\frac{34}{3}$	$\frac{20}{3}$
$(\mathbf{10}_4, \mathbf{1}_3)$	0	$\frac{8}{3}$	$\frac{20}{3}$	$-\frac{10}{3}$

TABLE XXVII. Matrix elements for **10** and $J = 3/2$. Eigenvalues: -12, 6, -2, -2.

$\mathbf{10}_4$	$(\mathbf{8}_2, \mathbf{8}_3)$	$(\mathbf{10}_4, \mathbf{8}_1)$	$(\mathbf{10}_4, \mathbf{8}_3)$	$(\mathbf{10}_4, \mathbf{1}_3)$
$(\mathbf{8}_2, \mathbf{8}_3)$	$\frac{2}{3}$	$2\sqrt{6}$	$-\frac{2\sqrt{10}}{3}$	$\frac{4\sqrt{10}}{3}$
$(\mathbf{10}_4, \mathbf{8}_1)$	$2\sqrt{6}$	-3	$\sqrt{15}$	0
$(\mathbf{10}_4, \mathbf{8}_3)$	$-\frac{2\sqrt{10}}{3}$	$\sqrt{15}$	$-\frac{19}{3}$	$\frac{8}{3}$
$(\mathbf{10}_4, \mathbf{1}_3)$	$\frac{4\sqrt{10}}{3}$	0	$\frac{8}{3}$	$-\frac{4}{3}$

TABLE XXVIII. Matrix elements for **10** and $J = 5/2$. Eigenvalues: 6, -2.

$\mathbf{10}_6$	$(\mathbf{10}_4, \mathbf{8}_3)$	$(\mathbf{10}_4, \mathbf{1}_3)$
$(\mathbf{10}_4, \mathbf{8}_3)$	2	-4
$(\mathbf{10}_4, \mathbf{1}_3)$	-4	2

TABLE XXIX. Matrix elements for $\mathbf{10}^*$ and $J = 1/2$. Eigenvalues: 6, -2.

$\mathbf{10}^*_2$	$(\mathbf{8}_2, \mathbf{8}_1)$	$(\mathbf{8}_2, \mathbf{8}_3)$
$(\mathbf{8}_2, \mathbf{8}_1)$	0	$2\sqrt{3}$
$(\mathbf{8}_2, \mathbf{8}_3)$	$2\sqrt{3}$	4

TABLE XXX. Matrix elements for $\mathbf{10}^*$ and $J = 3/2$. Eigenvalues: -2.

$\mathbf{10}^*_4$	$(\mathbf{8}_2, \mathbf{8}_3)$
$(\mathbf{8}_2, \mathbf{8}_3)$	-2

TABLE XXXI. Matrix elements for **27** and $J = 1/2$. Eigenvalues: 6, -2, -2.

$\mathbf{27}_2$	$(\mathbf{8}_2, \mathbf{8}_1)$	$(\mathbf{8}_2, \mathbf{8}_3)$	$(\mathbf{10}_4, \mathbf{8}_3)$
$(\mathbf{8}_2, \mathbf{8}_1)$	2	$-\frac{4}{\sqrt{3}}$	$4\sqrt{\frac{2}{3}}$
$(\mathbf{8}_2, \mathbf{8}_3)$	$-\frac{4}{\sqrt{3}}$	$-\frac{2}{3}$	$-\frac{4\sqrt{2}}{3}$
$(\mathbf{10}_4, \mathbf{8}_3)$	$4\sqrt{\frac{2}{3}}$	$-\frac{4\sqrt{2}}{3}$	$\frac{2}{3}$

TABLE XXXII. Matrix elements for **27** and $J = 3/2$. Eigenvalues: 6, -2, -2.

$\mathbf{27}_4$	$(\mathbf{8}_2, \mathbf{8}_3)$	$(\mathbf{10}_4, \mathbf{8}_1)$	$(\mathbf{10}_4, \mathbf{8}_3)$
$(\mathbf{8}_2, \mathbf{8}_3)$	$\frac{10}{3}$	$-\frac{4}{\sqrt{3}}$	$-\frac{4\sqrt{5}}{3}$
$(\mathbf{10}_4, \mathbf{8}_1)$	$-\frac{4}{\sqrt{3}}$	-1	$\sqrt{\frac{5}{3}}$
$(\mathbf{10}_4, \mathbf{8}_3)$	$-\frac{4\sqrt{5}}{3}$	$\sqrt{\frac{5}{3}}$	$-\frac{1}{3}$

TABLE XXXIII. Matrix elements for **27** and $J = 5/2$. Eigenvalues: -2.

$\mathbf{27}_6$	$(\mathbf{10}_4, \mathbf{8}_3)$
$(\mathbf{10}_4, \mathbf{8}_3)$	-2

TABLE XXXIV. Matrix elements for **35** and $J = 1/2$. Eigenvalues: -2.

$\mathbf{35}_2$	$(\mathbf{10}_4, \mathbf{8}_3)$
$(\mathbf{10}_4, \mathbf{8}_3)$	-2

TABLE XXXV. Matrix elements for **35** and $J = 3/2$. Eigenvalues: 6, -2.

$\mathbf{35}_4$	$(\mathbf{10}_4, \mathbf{8}_1)$	$(\mathbf{10}_4, \mathbf{8}_3)$
$(\mathbf{10}_4, \mathbf{8}_1)$	3	$-\sqrt{15}$
$(\mathbf{10}_4, \mathbf{8}_3)$	$-\sqrt{15}$	1

TABLE XXXVI. Matrix elements for **35** and $J = 5/2$. Eigenvalues: 6.

$\mathbf{35}_6$	$(\mathbf{10}_4, \mathbf{8}_3)$
$(\mathbf{10}_4, \mathbf{8}_3)$	6

be found in [62,66]. The tables of this Appendix can be obtained using the SU(6) $\supset$ SU(3) $\otimes$ SU(2) scalar factors in [62]. The same scalar factors but with the convention of [65] can be found in [67,68].

For instance, from [62,66] and including the appropriate spin SU(2) Clebsch-Gordan coefficients, we learn that

$$|N\bar{K}^*\rangle^{S=-1,I=1,J=3/2} = -\sqrt{\frac{3}{10}}|(\mathbf{8_2},\mathbf{8_3}),\mathbf{8_{s,4}}\rangle - \frac{1}{\sqrt{6}}|(\mathbf{8_2},\mathbf{8_3}),\mathbf{8_{a,4}}\rangle - \frac{1}{\sqrt{6}}|(\mathbf{8_2},\mathbf{8_3}),\mathbf{10_4}\rangle + \frac{1}{\sqrt{6}}|(\mathbf{8_2},\mathbf{8_3}),\mathbf{10_4^*}\rangle + \frac{1}{\sqrt{5}}|(\mathbf{8_2},\mathbf{8_3}),\mathbf{27_4}\rangle, \tag{A1}$$

$$|\Sigma^*\eta\rangle^{S=-1,I=1,J=3/2} = \frac{1}{\sqrt{5}}|(\mathbf{10_4},\mathbf{8_1}),\mathbf{8_4}\rangle + \sqrt{\frac{3}{10}}|(\mathbf{10_4},\mathbf{8_1}),\mathbf{27_4}\rangle + \frac{1}{\sqrt{2}}|(\mathbf{10_4},\mathbf{8_1}),\mathbf{35_4}\rangle.$$

Henceforth, using the tables provided for $\mathbf{8_4}$ and $\mathbf{27_4}$, one easily obtains

$$\begin{aligned}\xi^{-1,1,3/2}_{\Sigma^*\eta,N\bar{K}^*} &= \langle\Sigma^*\eta|\mathbf{8_4}\rangle\langle(\mathbf{10_4},\mathbf{8_1})|\xi^{\mathbf{8_4}}|(\mathbf{8_2},\mathbf{8_3})_s\rangle\langle\mathbf{8_{s,4}}|N\bar{K}^*\rangle + \langle\Sigma^*\eta|\mathbf{8_4}\rangle\langle(\mathbf{10_4},\mathbf{8_1})|\xi^{\mathbf{8_4}}|(\mathbf{8_2},\mathbf{8_3})_a\rangle\langle\mathbf{8_{a,4}}|N\bar{K}^*\rangle \\ &\quad + \langle\Sigma^*\eta|\mathbf{27_4}\rangle\langle(\mathbf{10_4},\mathbf{8_1})|\xi^{\mathbf{27_4}}|(\mathbf{8_2},\mathbf{8_3})\rangle\langle\mathbf{27_4}|N\bar{K}^*\rangle \\ &= \frac{1}{\sqrt{5}}\underbrace{(2\sqrt{3})}_{\text{Table XXIV}}\left(-\sqrt{\frac{3}{10}}\right) + \frac{1}{\sqrt{5}}\underbrace{(0)}_{\text{Table XXIV}}\left(-\sqrt{\frac{1}{6}}\right) + \sqrt{\frac{3}{10}}\underbrace{\left(-\frac{4}{\sqrt{3}}\right)}_{\text{Table XXXII}}\frac{1}{\sqrt{5}} = -\sqrt{2}.\end{aligned} \tag{A2}$$

APPENDIX B: πN S_{11} PHASE SHIFT AND INELASTICITIES

In this appendix, we pay special attention to πN elastic and inelastic scattering, and, in particular, to phase shifts, inelasticities and some total inelastic cross sections in the S_{11} wave (notation L_{2I2J}, with L the πN orbital angular momentum). We will restrict our discussion to relatively low energies ($\sqrt{s} < 1.7$ GeV), where the $N(1535)$ and $N(1650)$ four star resonances generated by the interaction in the 56 and 70 irreps should play a central role. Phase shifts, inelasticities and inelastic cross sections are evaluated using Eqs. (18), (19) and (35) of Ref. [20], but replacing this latter equation by

$$[f_0^{1/2}(s)]_{BA} = -\frac{1}{8\pi\sqrt{s}}\sqrt{\frac{|\vec{k}_B|}{|\vec{k}_A|}}\frac{T_{BA}}{\sqrt{2M_A}\sqrt{2M_B}}, \tag{B1}$$

for the transition $B \leftarrow A$. This is necessary to account for minor differences between the normalizations used here and those employed in [20].

At first sight, the model presented up to here (solid lines in Fig. 4, labeled model 0 there) leads to a poor description of data, though it already explains their gross features.[13] Indeed, we could appreciate the changes of curvarture in the phase-shifts and inelasticities, which hints the existence of both the $N(1535)$ and $N(1650)$ resonances. Those states show clearly up in the $\pi^- p \to \eta n$ and $\pi^- p \to K^0\Lambda$ total cross sections, as well.

This raw description of the data should not be surprising, since we have not fitted any parameter and we have just retained here the SU(3) WT lowest order contribution to fix the SU(6) interaction. Accurate descriptions of data have been achieved in previous works [20,27,49], but always within more general schemes, where a large number of parameters are fitted to data. Thus for instance in [20], though vector meson and decuplet baryon degrees of freedom are not incorporated and the SU(3) WT is taken as the kernel to solve a Bethe-Salpeter equation (BSE), the consideration of off-shell effects in [20] led to a total of 12 counterterms which are fitted to data. Four of them (one for each of the four channels, πN, ηN, $K\Lambda$ and $K\Sigma$, included in [20]) are the subtraction constants needed in Eq. (14) to renormalize the ultraviolet divergences in the loop function. Here, we have not only neglected the counterterms that arise from off-shell effects in the solution of the BSE, moreover, those counterterms that appear in the on-shell scheme adopted here have also been totally fixed, by means of the prescription of Eq. (15), instead of fitting them to data. In Ref. [49], there is a total of 17 free parameters, given by the 14 low energy constants that appear when one goes beyond the SU(3) WT term, and includes all dimension two contact terms, as well as three subtraction constants for the regularized loop integrals.[14] Finally, in [27] an even larger number of parameters is fitted to data.

We could adopt here also a more flexible RS, and relax the prescription of Eq. (15) to achieve a better agreement to data. Fitting the subtraction constants to data is a difficult task, since there are likely many local minima, and it requires a careful analysis. Besides, it would also require working in parallel possible off-shell effects [20] and next-to-leading contributions [49] to the kernel of the BSE.

[13] Note that we do not show results for the $\pi^- p \to K^0\Sigma^0$ total cross section because of the likely sizable isospin 3/2 contribution, and that as the C.M. energy increases, higher πN wave contributions (neglected here) to the two total inelastic cross sections shown in Fig. 4 become much more relevant. Yet the three-body final state $\pi N \to N\pi\pi$ process, not considered here, will affect to the inelasticities, as well [19,20].

[14] In [49], it is assumed the same subtraction constant for both the $K\Lambda$ and $K\Sigma$ channels.

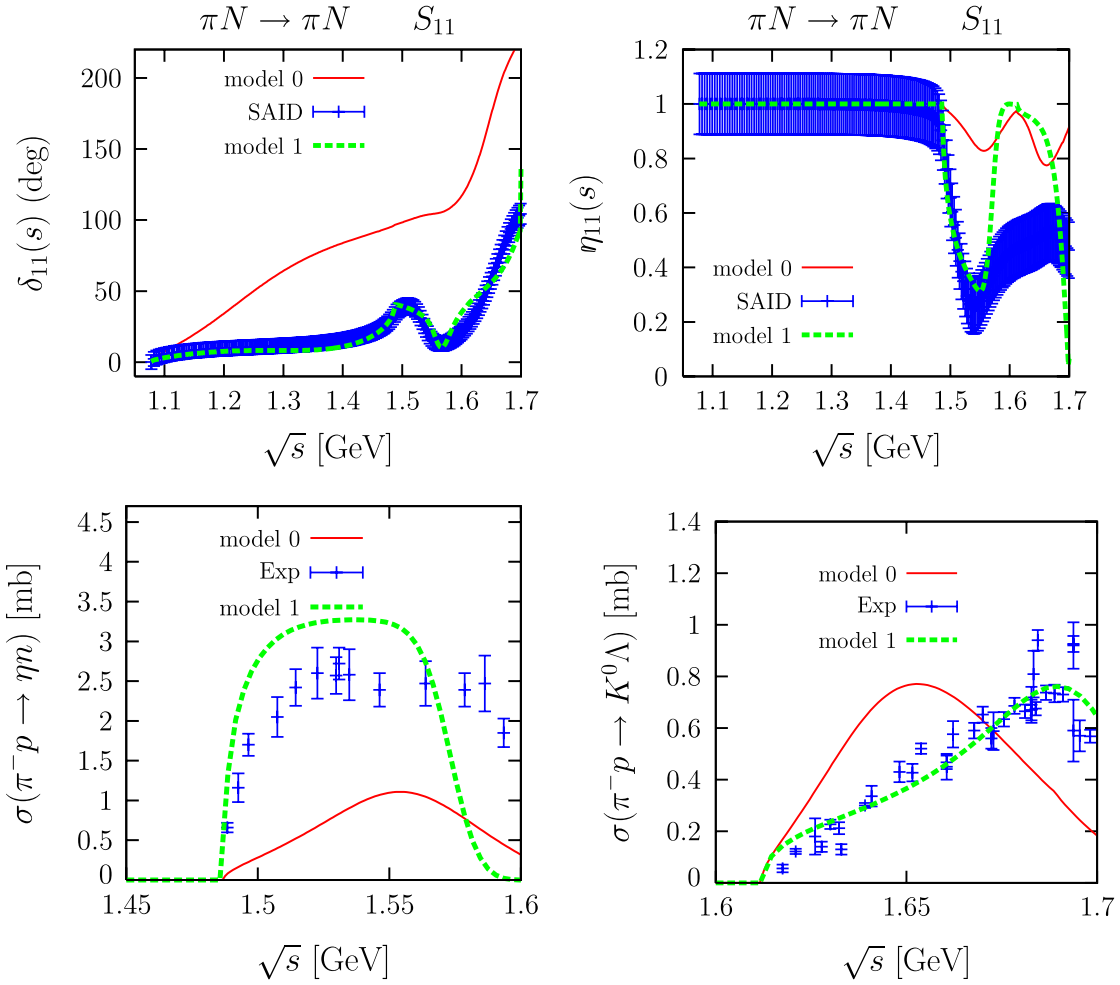

FIG. 4 (color online). Top panels: S_{11} elastic πN phase shifts (left) and inelasticities (right) as a function of the C.M. energy $\sqrt{s}$. Data are from Ref. [69], and to better appreciate the discrepancies, we have assumed in both cases a 5% systematic error and a statistical uncertainty of 5° and 0.1 for $\delta's$ and $\eta's$, respectively, (errors have been added in quadrature). Bottom panels: $\pi^- p \to \eta n$ and $\pi^- p \to K^0 \Lambda$ total cross sections as a function of $\sqrt{s}$. Data are from Ref. [70]. Solid lines (model 0) stand for the predictions obtained within the scheme presented here, where no parameters have been adjusted to data. Dashed lines (model 1) show results from a modified model, where in Eq. (14), the subtraction constants $\bar{J}_0(\mu = \sqrt{m_\pi^2 + M_N^2}; M_i, m_i))$ are multiplied by the factors -0.039, 0.007, 2.228, -0.539, 0.443, 0.757, 2.855, 0.710, 1.460, 2.677, 0.333, for the πN, ηN, $K\Lambda$, $K\Sigma$, ρN, ωN, ϕN, $\rho\Delta$, $K^*\Lambda$, $K^*\Sigma$, $K^*\Sigma^*$ channels, respectively.

These latter ones should account also for additional SU(6) and SU(3) breaking terms to be considered on top of those already incorporated in our simplified scheme. This is an ambitious and formidable task, which is out of the scope of the present work. Here, we just aim to show how the underlying chiral symmetry of the WT term induces a qualitative SU(6) classification pattern, where most of the lowest-lying odd-parity three and four star resonances of the PDG fill into 70 and 56 irrep SU(6) multiplets. We would like however to point out that there are regions in the parameter space which lead to better descriptions of the scattering data. As a matter of example, we also show in Fig. 4, results (dashed lines, labeled model 1 there) which look more phenomenologically acceptable, and have been obtained by modifying the prescription of Eq. (15) (see figure caption, for more details.[15]) For this particular set of parameters the state identified with the $N(1535)$ becomes wider whereas that identified with the $N(1650)$ becomes lighter than the corresponding states in the model 0.

The conclusions of the above discussion are similar for other sectors of strangeness, spin and isospin.

In summary, the simple scheme advocated in this work, where no parameters are being fitted, provides the main features of the lowest-lying odd-parity baryon resonances.

[15]In some cases, there appear large deviations when compared to the prescription of Eq. (15), which however do not attribute much physical relevance, because of the complexity of the parameter space, as we already mentioned.

However, one should not expect a very good, actually it could be poor, description of data that, however, hints at their major features. This situation is similar for other simple models, like those of Refs. [22,25,26,28], where the Δ baryon decuplet and the vector meson nonet degrees of freedom are taken into account. Accurate descriptions of data, beyond masses, widths and the main couplings of the relevant low-lying resonances in each sector, can be achieved, but it requires much more physics to enter in the form of undetermined counterterms.

[1] K.-T. Chao, N. Isgur, and G. Karl, Phys. Rev. D **23**, 155 (1981).
[2] S. Capstick and N. Isgur, Phys. Rev. D **34**, 2809 (1986).
[3] L. Y. Glozman, W. Plessas, K. Varga, and R. F. Wagenbrunn, Phys. Rev. D **58**, 094030 (1998).
[4] A. Valcarce, H. Garcilazo, and J. Vijande, Phys. Rev. C **72**, 025206 (2005).
[5] C. E. Carlson and C. D. Carone, Phys. Lett. B **484**, 260 (2000).
[6] C. L. Schat, J. L. Goity, and N. N. Scoccola, Phys. Rev. Lett. **88**, 102002 (2002).
[7] J. L. Goity, C. Schat, and N. N. Scoccola, Phys. Lett. B **564**, 83 (2003).
[8] N. Matagne and F. Stancu, Phys. Rev. D **71**, 014010 (2005).
[9] R. Bijker, F. Iachello, and A. Leviatan, Ann. Phys. (N.Y.) **284**, 89 (2000).
[10] D. Jido and M. Oka, arXiv:hep-ph/9611322v2.
[11] Y. Oh, Phys. Rev. D **75**, 074002 (2007).
[12] E. Oset and A. Ramos, Nucl. Phys. **A635**, 99 (1998).
[13] J. A. Oller and U. G. Meissner, Phys. Lett. B **500**, 263 (2001).
[14] C. Garcia-Recio, J. Nieves, E. Ruiz Arriola, and M. J. Vicente Vacas, Phys. Rev. D **67**, 076009 (2003).
[15] C. Garcia-Recio, M. F. M. Lutz, and J. Nieves, Phys. Lett. B **582**, 49 (2004).
[16] O. Krehl, C. Hanhart, S. Krewald, and J. Speth, Phys. Rev. C **62**, 025207 (2000).
[17] N. Kaiser, P. B. Siegel, and W. Weise, Nucl. Phys. **A594**, 325 (1995).
[18] N. Kaiser, P. B. Siegel, and W. Weise, Phys. Lett. B **362**, 23 (1995).
[19] T. Inoue, E. Oset, and M. J. Vicente Vacas, Phys. Rev. C **65**, 035204 (2002).
[20] J. Nieves and E. Ruiz Arriola, Phys. Rev. D **64**, 116008 (2001).
[21] E. E. Kolomeitsev and M. F. M. Lutz, Phys. Lett. B **585**, 243 (2004).
[22] S. Sarkar, E. Oset, and M. J. Vicente Vacas, Nucl. Phys. **A750**, 294 (2005); **A780**, 90(E) (2006).
[23] M. Bando, T. Kugo, S. Uehara, K. Yamawaki, and T. Yanagida, Phys. Rev. Lett. **54**, 1215 (1985).
[24] M. Bando, T. Kugo, and K. Yamawaki, Phys. Rep. **164**, 217 (1988).
[25] P. Gonzalez, E. Oset, and J. Vijande, Phys. Rev. C **79**, 025209 (2009).
[26] S. Sarkar, B. X. Sun, E. Oset, and M. J. V. Vacas, Eur. Phys. J. A **44**, 431 (2010).
[27] M. F. M. Lutz, G. Wolf, and B. Friman, Nucl. Phys. **A706**, 431 (2002).
[28] E. Oset and A. Ramos, Eur. Phys. J. A **44**, 445 (2010).
[29] C. Garcia-Recio, L. S. Geng, J. Nieves, and L. L. Salcedo, Phys. Rev. D **83**, 016007 (2011).
[30] B. Aubert *et al.* (BABAR Collaboration), Phys. Rev. D **78**, 034008 (2008).
[31] C. Garcia-Recio, J. Nieves, and L. L. Salcedo, Phys. Rev. D **74**, 034025 (2006).
[32] C. Garcia-Recio, J. Nieves, and L. L. Salcedo, Phys. Rev. D **74**, 036004 (2006).
[33] C. Garcia-Recio, J. Nieves, and L. L. Salcedo, Eur. Phys. J. A **31**, 499 (2007).
[34] D. G. Caldi and H. Pagels, Phys. Rev. D **14**, 809 (1976); **15**, 2668 (1977).
[35] R. P. Feynman, M. Gell-Mann, and G. Zweig, Phys. Rev. Lett. **13**, 678 (1964).
[36] D. Gamermann, C. Garcia-Recio, J. Nieves, L. L. Salcedo, and L. Tolos, Phys. Rev. D **81**, 094016 (2010).
[37] C. Garcia-Recio, V. K. Magas, T. Mizutani, J. Nieves, A. Ramos, L. L. Salcedo, and L. Tolos, Phys. Rev. D **79**, 054004 (2009).
[38] J. Hofmann and M. F. M. Lutz, Nucl. Phys. **A763**, 90 (2005).
[39] J. Hofmann and M. F. M. Lutz, Nucl. Phys. **A776**, 17 (2006).
[40] L. Roca, S. Sarkar, V. K. Magas, and E. Oset, Phys. Rev. C **73**, 045208 (2006).
[41] D. Gamermann and E. Oset, Eur. Phys. J. A **33**, 119 (2007).
[42] S. Weinberg, Phys. Rev. Lett. **17**, 616 (1966).
[43] Y. Tomozawa, Nuovo Cimento A **46**, 707 (1966).
[44] E. Oset, A. Ramos, and C. Bennhold, Phys. Lett. B **527**, 99 (2002).
[45] K. Nakamura *et al.* (Particle Data Group), J. Phys. G **37**, 075021 (2010).
[46] R. A. Arndt, W. J. Briscoe, I. I. Strakovsky, and R. L. Workman, Phys. Rev. C **74**, 045205 (2006).
[47] T. P. Vrana, S. A. Dytman, and T. S. H. Lee, Phys. Rep. **328**, 181 (2000).
[48] R. E. Cutkosky, C. P. Forsyth, R. L. Kelly, and R. E. Hendrick, Phys. Rev. D **20**, 2839 (1979); R. E. Cutkosky, C. P. Forsyth, J. B. Babcock, R. L. Kelly, and R. E. Hendrick, in *Proceedings of the IV International Conference on Baryon Resonances, Baryon 1980, Toronto, Canada, 1980*, edited by N. Isgur (University of Toronto, Toronto, 1980), p. 19.
[49] P. C. Bruns, M. Mai, and U. G. Meissner, Phys. Lett. B **697**, 254 (2011).

[50] M. F. M. Lutz and E. E. Kolomeitsev, Nucl. Phys. **A700**, 193 (2002).
[51] J. J. Xie and J. Nieves, Phys. Rev. C **82**, 045205 (2010).
[52] N. Muramatsu *et al.*, Phys. Rev. Lett. **103**, 012001 (2009).
[53] H. Kohri *et al.* (LEPS Collaboration), Phys. Rev. Lett. **104**, 172001 (2010).
[54] A. d. Bellefon, A. Berthon, and P. Billoir, Nuovo Cimento Soc. Ital. Fis. A **28**, 289 (1975).
[55] S. Sarkar, E. Oset, and M. J. Vicente Vacas, Phys. Rev. C **72**, 015206 (2005).
[56] H. Toki, C. Garcia-Recio, and J. Nieves, Phys. Rev. D **77**, 034001 (2008).
[57] A. Ramos, E. Oset, and C. Bennhold, Phys. Rev. Lett. **89**, 252001 (2002).
[58] S. M. Flatte, Phys. Lett. B **63**, 224 (1976).
[59] N. P. Samios, M. Goldberg, and B. T. Meadows, Rev. Mod. Phys. **46**, 49 (1974).
[60] C. Garcia-Recio, J. Nieves, and L. L. Salcedo, Eur. Phys. J. A **31**, 540 (2007).
[61] D. Gamermann, J. Nieves, E. Oset, and E. Ruiz Arriola, Phys. Rev. D **81**, 014029 (2010).
[62] C. Garcia-Recio and L. L. Salcedo, J. Math. Phys. (N.Y.) **52**, 043503 (2011).
[63] A. J. G. Hey and R. L. Kelly, Phys. Rep. **96**, 71 (1983).
[64] G. E. Baird and L. C. Biedenharn, J. Math. Phys. (N.Y.) **5**, 1723 (1964).
[65] J. J. de Swart, Rev. Mod. Phys. **35**, 916 (1963); **37**, 326(E) (1965).
[66] V. Rabl, G. J. Campbell, and K. C. Wali, J. Math. Phys. (N.Y.) **16**, 2494 (1975); E. M. Haacke, J. W. Moffat, and P. Savaria, J. Math. Phys. (N.Y.) **17**, 2041 (1976).
[67] J. C. Carter, J. J. Coyne, and S. Meshkov, Phys. Rev. Lett. **14**, 523 (1965); **14**, 850(E) (1965).
[68] C. L. Cook and G. Murtaza, Nuovo Cimento **39**, 531 (1965).
[69] R. A. Arndt, I. I. Strakovsky, R. L. Workman, and M. M. Pavan, Phys. Rev. C **52**, 2120 (1995).
[70] A. Baldini *et al.*, in *Total Cross-Sections for Reactions of High Energy Particles: Including Elastic, Topological, Inclusive and Exclusive Reactions*, edited by H. Schopper, Landolt-Bornstein: Numerical Data and Functional Relationships in Science and Technology: New Series. Group I, Nuclear and Particle Physics Vol. 12a (Springer, Berlin, 1988).